Transcriptomic analysis of mRNA expression and alternative splicing during mouse sex determination

Zhao, Liang; Wang, Chenwei; Lehman, Melanie L.; He, Mingyu; An, Jiyuan; Svingen, Terje; Spiller, Cassy M.; Ng, Ee Ting; Nelson, Colleen C.; Koopman, Peter

Published in:
Molecular and Cellular Endocrinology

Link to article, DOI:
10.1016/j.mce.2018.07.010

Publication date:
2018

Document Version
Peer reviewed version

Accepted Manuscript

Transcriptomic analysis of mRNA expression and alternative splicing during mouse sex determination

Liang Zhao, Chenwei Wang, Melanie L. Lehman, Mingyu He, Jiyuan An, Terje Svingen, Cassy M. Spiller, Ee Ting Ng, Colleen C. Nelson, Peter Koopman

PII: S0303-7207(18)30234-X

DOI: 10.1016/j.mce.2018.07.010

Reference: MCE 10277

To appear in: *Molecular and Cellular Endocrinology*

Received Date: 17 May 2018

Revised Date: 23 July 2018

Accepted Date: 23 July 2018

Please cite this article as: Zhao, L., Wang, C., Lehman, M.L., He, M., An, J., Svingen, T., Spiller, C.M., Ng, E.T., Nelson, C.C., Koopman, P., Transcriptomic analysis of mRNA expression and alternative splicing during mouse sex determination, *Molecular and Cellular Endocrinology* (2018), doi: 10.1016/j.mce.2018.07.010.

Transcriptomic analysis of mRNA expression and alternative splicing during mouse sex determination

Liang Zhao,[1] Chenwei Wang,[2] Melanie L. Lehman,[2] Mingyu He[3], Jiyuan An,[2,4] Terje Svingen,[1,5] Cassy M. Spiller,[1,6] Ee Ting Ng,[1] Colleen C. Nelson,[2] and Peter Koopman[1*]

[1]Institute for Molecular Bioscience, The University of Queensland, Brisbane, Queensland 4072, Australia; [2]Australian Prostate Cancer Research Centre – Queensland, Institute of Health and Biomedical Innovation, Queensland University of Technology, Princess Alexandra Hospital, Translational Research Institute, Brisbane, Queensland 4102, Australia; [3]Longsoft, Brisbane, Queensland 4109, Australia

Corresponding author: Professor Peter Koopman, PhD, Institute for Molecular Bioscience, The University of Queensland, Brisbane, QLD 4072, Australia. Email: p.koopman@imb.uq.edu.au

Present address: J. An, QIMR Berghofer Medical Research Institute, Brisbane, Queensland 4006, Australia; T. Svingen, National Food Institute, Technical University of Denmark, Søborg 2860, Denmark; C. M. Spiller, School of Biomedical Sciences, The University of Queensland, Brisbane, Queensland 4072, Australia

ABSTRACT

Mammalian sex determination hinges on sexually dimorphic transcriptional programs in developing fetal gonads. A comprehensive view of these programs is crucial for understanding the normal development of fetal testes and ovaries and the etiology of human disorders of sex development (DSDs), many of which remain unexplained. Using strand-specific RNA-sequencing, we characterized the mouse fetal gonadal transcriptome from 10.5 to 13.5 days post coitum, a key time window in sex determination and gonad development. Our dataset benefits from a greater sensitivity, accuracy and dynamic range compared to microarray studies, allows global dynamics and sex-specificity of gene expression to be assessed, and provides a window to non-transcriptional events such as alternative splicing. Spliceomic analysis uncovered female-specific regulation of *Lef1* splicing, which may contribute to the enhanced WNT signaling activity in XX gonads. We provide a user-friendly visualization tool for the complete transcriptomic and spliceomic dataset as a resource for the field.

Keywords: RNA-Seq, gonadal development, transcriptional regulation, *Lef1*, testis, ovary

1. Introduction

In eutherian mammals, sex differentiation stems from a critical decision made in the bipotential fetal genital ridges whether to adopt a testicular or ovarian fate. In the presence of a Y chromosome, the expression of the Y-linked transcription factor SRY (sex-determining region Y) in the indifferent genital ridges activates its target gene Sox9 (SRY-box 9), also encoding a transcription factor, which subsequently drives and coordinates the cascade of gene expression leading to the formation of fetal testes (Koopman et al., 1991; Li et al., 2014; Rahmoun et al., 2017; Sekido and Lovell-Badge, 2008; Vidal et al., 2001). In the absence of SRY, RSPO1 (R-spondin 1)/WNT4 (wingless-type MMTV integration site family, member 4)/ CTNNB1 (catenin, beta 1) and FOXL2 (forkhead box L2) induce an alternative set of transcriptional programs, giving rise to fetal ovaries (Chassot et al., 2008; Liu et al., 2009; Ottolenghi et al., 2007; Schmidt et al., 2004; Uda et al., 2004; Vainio et al., 1999). The sex-specific pathways antagonize each other to secure the chosen sexual fate and repress the alternative fate (Bagheri-Fam et al., 2017; Chang et al., 2008; Greenfield, 2015; Jameson et al., 2012a; Kashimada et al., 2011; Kim et al., 2006; Maatouk et al., 2008; Wilhelm et al., 2009). However, two major bottlenecks in our understanding of how sex determination and gonadal differentiation are controlled at the molecular genetic level are the identification of new genes and an appreciation of how they are coordinately regulated. As a result, we lack an explanation for the majority of the large suite of human anatomical variations that are collectively described as disorders of sex development (DSDs) (Eggers et al., 2016).

To address the bottlenecks, a number of genome-wide expression studies have been conducted either on mouse or human whole fetal gonads (Del Valle et al., 2017; Houmard et al., 2009; Munger et al., 2013; Rahmoun et al., 2017; Rolland et al., 2011; Small et al., 2005)

or isolated fetal gonadal cell populations (Beverdam and Koopman, 2006; Bouma et al., 2007; Bouma et al., 2010; Inoue et al., 2016; Jameson et al., 2012b; McClelland et al., 2015; Nef et al., 2005). Most of these studies were performed using microarray technology (Beverdam and Koopman, 2006; Bouma et al., 2007; Bouma et al., 2010; Del Valle et al., 2017; Houmard et al., 2009; Jameson et al., 2012b; Munger et al., 2013; Nef et al., 2005; Rolland et al., 2011; Small et al., 2005). While these continue to serve as valuable resources for the field, microarray studies are limited by technical issues, including limited probe coverage, inconsistent probe hybridization efficiency, relatively low sensitivity and narrow dynamic range, and limited ability to distinguish transcript isoforms on a global scale (Zhao et al., 2014).

Alternatively, RNA-sequencing (RNA-Seq) can be used to circumvent these issues. Two RNA-Seq studies have investigated the transcriptome of a specific cell lineage, the fetal Leydig cell (Inoue et al., 2016; McClelland et al., 2015), while a third has used chromatin immunoprecipitation followed by RNA-Seq (ChIP-Seq) to characterize the regulome of the key gonadal transcription factor SOX9 (Rahmoun et al., 2017). More recently, a single-cell RNA-Seq study (Stévant et al., 2018) has been performed to provide new insights into the transcriptional variability between cells, and investigate lineage relationships in the developing gonads. Although single cell sequencing holds great potential for further investigations, it is currently limited in its ability to illuminate some poorly understood areas such as the role of alternative splicing and its regulation (Haque et al., 2017). As such, there remains an important place for RNA-seq analyses of whole-organ development.

In the present study, we employed a strand-specific RNA-Seq strategy to analyze the transcriptome of the mouse developing fetal testes and ovaries at key developmental stages encompassing the period from *Sry* activation in the male to differentiation and early histological arrangement of the gonadal cell lineages. Our results provide a comprehensive view of the transcriptional events at both the gene and transcript level underlying sexual fate commitment and fetal gonadal development. Furthermore, our analyses uncovered widespread spatio-temporal regulation of transcript isoform usage in the fetal gonads, suggesting an important regulatory role of alternative splicing in these processes.

2. Materials and methods

2.1 Mice and tissue collection

A reporter mouse line carrying an X-linked GFP transgene (XGFP) (Hadjantonakis et al., 1998) was used to facilitate non-invasive sexing: $X^{GFP}Y$ studs were mated to outbred Swiss albino (Quakenbush) XX females to generate timed pregnancies, with noon of the day on which the mating plug was observed designated as 0.5 days post coitum (dpc). Embryos at 10.5 or 11.5 dpc were sexed using a Leica M165 FC fluorescent stereomicroscope based on GFP expression in $X^{GFP}X$ embryos; embryos at 12.5 or 13.5 dpc were sexed by visual inspection of the fetal gonads. To ensure correct staging at 10.5 and 11.5 dpc, tail somites (ts) were counted as described (Hacker et al., 1995). Genital ridges/fetal gonads at 10.5 (ts 7–9), 11.5 (ts17–19), 12.5 or 13.5 dpc were dissected in cold PBS (Life Tech) with mesonephros removed. Although we took extra care dissecting genital ridges at 10.5 dpc, cross contamination of genital ridges by mesonephric tissue cannot be completely ruled out. Gonadal tissues from multiple embryos were pooled to obtain enough RNA for sequencing: 30–40, 20–30, 5–10, or 3–8 pairs of fetal gonads were pooled at 10.5, 11.5, 12.5 or 13.5 dpc,

respectively. For each sex and time point, two independent tissue pools were collected as biological duplicate samples. An additional tissue pool of 13.5-dpc ovaries was collected to facilitate between-batch normalization (see below). All animal experimentation was approved (permits IMB/230/12 and IMB/175/13) and carried out according to the guidelines established by the University of Queensland Animal Ethics Committee.

2.2 RNA extraction and sequencing

Total RNA was extracted using Qiagen RNeasy Micro kit with on-column DNase I treatment and sequenced at Macrogen (Seoul, Korea). Briefly, strand-specific sequencing libraries were prepared from polyA-enriched mRNA using a ScriptSeq mRNA-Seq library preparation kit (EpiCentre). Sequencing libraries were prepared in two batches, with the second batch samples labelled with a suffix “new” (Supplemental Table S1). Libraries were multiplexed (4 on each lane) and sequenced on an Illumina HiSeq2000. An extra 13.5-dpc XX RNA sample, 13.5F3new, was sequenced to facilitate normalization between batches, and subsequently included in downstream analyses as an additional biological replicate. Sequencing of sample 11.5M1 (11.5-dpc XY pool #1) failed, as indicated by a very low overall read alignment rate (< 20%; data not shown); it was therefore excluded from further analysis. Data have been deposited to SRA under the accession number SRP076584.

2.3 Differential expression analysis at the gene or transcript level

Sequencing reads were trimmed with Trimmomatic (Bolger et al., 2014) v0.20 and aligned to annotated genes or transcripts in mouse Ensembl 75 reference transcriptome using the RSEM algorithm (Li and Dewey, 2011) v1.2.12. Between-sample TMM (trimmed mean of M values)

normalization was carried out as described (Robinson and Oshlack, 2010). Differential expression analysis at the gene level was performed on pairwise comparisons of samples between the two sexes at the same time point or between two consecutive time points of the same sex using edgeR (Robinson et al., 2010) v3.6.2, with a batch component added to the generalized linear model (log-ratio test) where applicable. edgeR uses empirical Bayes methods that enable sharing of information between genes, thereby allowing estimation of gene-specific biological variation even when only a limited number of biological replicates are available (McCarthy et al., 2012).

Differentially expressed genes (DEGs) were determined as those with an adjusted *P* value < 0.05. Pathway analysis of DEGs was performed using Qiagen's Ingenuity Pathway Analysis (IPA) tool v. 36601845. For cross-comparisons with other datasets, genes with multiple Ensembl Gene IDs were consolidated. Area proportional Venn diagrams were generated using BioVenn (Hulsen et al., 2008).

Differential expression analysis at the transcript level was performed similarly as the gene-level analysis. As the distribution of reads among transcript isoforms by RSEM may not be accurate for those expressed at low levels (Zhao et al., 2015), we filtered the dataset to remove transcripts with very low expression and low isoform percentage using a cut-off of TPM (transcripts per million) expression > 5 and isoform percentage > 10% in 11.5M2 sample (as only one 11.5-dpc XY sample is available) or at least two other samples.

We provide TPM expression values for all genes with detectable expression (RSEM expected counts > 0) and filtered transcripts in Supplemental Tables S2 and S6 respectively, along with edgeR statistical test results (log_2 fold change and adjusted *P* values). A graphing tool for visualization of the expression of any chosen gene or transcript over the time course was also included.

2.4 Co-expression gene network analysis

A signed weighted gene correlation network analysis was carried out using the WGCNA package (Langfelder and Horvath, 2008; Zhang and Horvath, 2005) on log-transformed FPKM (fragments per kilobase per million) values (provided in Supplemental Table S2). To restrict noise and for computational convenience, we performed the analysis on 8966 genes abundantly expressed in mouse fetal gonads during the time course (FPKM > 10 in at least 1 sample). Genes were clustered using a hierarchical clustering algorithm based on topological overlap distance. The branches representing highly co-expressed genes were then identified with a Dynamic Tree Cut approach. These initial groups of co-expressed genes were further merged to form the final gene modules according to their co-expression similarity (correlation coefficient ≥ 0.85) measured by their eigengenes (i.e. principal components).

Gene modules significantly correlated with various traits (combinations of sex and developmental stage) were identified using Pearson's correlation analysis. We included two additional traits (12.5+13.5 dpc XX and 12.5+13.5 dpc XY) in the module-trait correlation analysis to facilitate the identification of modules expressed at similar levels at 12.5 and 13.5 dpc. Significant gene modules were identified with a threshold of the absolute value of

Pearson's correlation coefficient ≥ 0.65 and a correlation test *P* value ≤ 0.05. These modules were then analyzed for enriched pathway terms using IPA v. 36601845.

2.5 Differential splicing analysis

Sequencing reads were mapped to the mouse reference genome assembly GRCm38/mm10 (with Ensembl 75 annotated transcript junctions) using STAR aligner (Dobin et al., 2013) v2.4.0.1 with default settings. Differential exon usage was analyzed using DEXSeq (Anders et al., 2012) v1.22.0, with a batch component added to the generalized linear model where applicable. Differentially spliced exonic regions were determined as those with an adjusted *P* value < 0.05 and $\log_2$ fold change > 1 or < -1.

3. Results

3.1 RNA-Seq analysis, data visualization and validation

We performed strand-specific RNA-Seq on pooled mouse XX or XY genital ridges/fetal gonads (with mesonephroi removed) at four time points, namely 10.5, 11.5, 12.5 and 13.5 dpc, encompassing the critical period during which the bi-potential genital ridges form, sex is determined, and the gonads differentiate to either fetal testes or ovaries (Fig. 1). Strand-specific libraries were prepared from duplicate RNA pools of XX or XY fetal gonads at each time point and sequenced on the Illumina platform (data accessible at SRA; SRP076584). An additional 13.5-dpc XX gonad sample pool was included to facilitate normalization. On average, ~40–50 million stranded 101-bp paired-end sequencing reads were generated from each sample (Supplemental Table S1). After trimming, reads were mapped to the mouse Ensembl 75 reference transcriptome, and gene expression levels (TPM, transcripts per million) were estimated using the RSEM algorithm (Li and Dewey, 2011). On average, ~30 million reads of each sample were aligned (overall read alignment rate ~60–70%; Supplemental Table S1), except sample 11.5M1 which has an alignment rate <20% (data not shown) and was therefore excluded from further analyses.

In total, we detected expression of 26,660 genes in the developing mouse fetal gonads during the time course (RSEM counts of assigned reads >0 in at least one sample). We provide TPM expression values and statistics values from differential expression analysis (see below) for all detected genes in a spreadsheet format (Supplemental Table S2) as a resource for the community.

To further enhance the utility of this resource, we include a graphing tool for visualizing the expression profile of any given gene over the time course (similar to that provided in ref. (Jameson et al., 2012b)). Instructions for using this tool can be found in the legend to Supplemental Table S2. The expression graphs shown in Fig. 2 and Supplemental Fig. S2 were generated using this graphing tool.

To validate the data, we first performed an unsupervised clustering analysis using multi-dimensional scaling analysis (Robinson et al., 2010). As expected, biological replicates clustered tightly by stage and sex (Supplemental Fig. S1) (Jameson et al., 2012b; Munger et al., 2013), confirming the quality of the data. We further validated the RNA-Seq data by examining the expression patterns of established marker genes for sex determination and/or fetal gonadal development. *Sry* showed a transient expression peak at 11.5 dpc (Fig. 2), consistent with in-situ hybridization and real-time PCR analyses (Bullejos and Koopman, 2001; Hacker et al., 1995; Jeske et al., 1996; Koopman et al., 1990; Wilhelm et al., 2005). Similarly, transcriptional profiles of many other known important genes in the RNA-Seq data were consistent with their documented expression patterns (Fig. 2 and Supplemental Fig. S2), reflecting the quality of our data; these known genes include markers for differentiation of Sertoli cells (*Sox9* (da Silva et al., 1996; Kent et al., 1996), *Amh* (anti-Mullerian hormone) (Munsterberg and Lovell-Badge, 1991), *Fgf9* (fibroblast growth factor 9) (Colvin et al., 2001), *Dhh* (desert hedgehog) (Bitgood et al., 1996) and *Ptgds* (prostaglandin D2 synthase) (Adams and McLaren, 2002)), granulosa cells (*Rspo1* (Parma et al., 2006), *Foxl2* (Loffler et al., 2003), *Wnt4* (Vainio et al., 1999), *Irx3* (Iroquois related homeobox 3) (Jorgensen and Gao, 2005), *Bmp2* (bone morphogenetic protein 2) (Yao et al., 2004) and *Fst* (follistatin) (Menke and Page, 2002; Yao et al., 2004)), fetal Leydig cell (*Insl3* (insulin like 3) (Zimmermann et al., 1997), *Hsd3b1* (hydroxy-delta-5-steroid dehydrogenase, 3 beta- and steroid delta-

isomerase 1) (Baker et al., 1999), *Star* (steroidogenic acute regulatory protein) (Odet et al., 2004) and *Cyp11a1* (cytochrome P450, family 11, subfamily a, polypeptide 1) (Ikeda et al., 1994)), and male or female germ cells (*Nanos2* (nanos C2HC-type zinc finger 2) (Tsuda et al., 2003), *Nodal*, *Lefty1* (left right determination factor 1) (Spiller et al., 2012), *Msx1* (msh homeobox 1) (Le Bouffant et al., 2011), *Stra8* (stimulated by retinoic acid gene 8) and *Dmc1* (DNA meiotic recombinase 1) (Menke et al., 2003)).

3.2 Male *vs.* female comparison

We performed differential expression analysis to identify genes expressed in a sex-dependent manner using the edgeR algorithm (Robinson et al., 2010), and identified thousands of genes manifesting sexually dimorphic expression over the time course (adjusted P value < 0.05; Fig. 3A and Supplemental Table S3). At 10.5 dpc, we found a very small number of genes with sex-biased expression, consistent with a previous report (Nef et al., 2005). Nine genes were expressed at levels higher in XY genital ridges, including *Sry*, which was expressed at low but detectable levels (Supplemental Table S2). Five genes showed female-biased expression, including *Xist* (inactive X specific transcripts), involved in X-inactivation (Brown et al., 1991). As expected, most sexually dimorphic genes at this stage were either X- or Y-linked (Fig. 3A and Supplemental Table S3), in accordance with the indifferent nature of the genital ridges at this time point.

Sexually dimorphic gene expression began in the fetal gonads during sex determination at 11.5 dpc, with 108 genes becoming differentially expressed before overt morphological changes arise (Fig. 3A and Supplemental Tables S3). Among 9 female-biased genes were

Foxl2 and *Fst*, two genes known to play important roles in ovarian development and maintenance (Schmidt et al., 2004; Uda et al., 2004; Uhlenhaut et al., 2009; Yao et al., 2004). Of the 99 male-biased genes, many play critical roles in male sex determination and/or fetal testis development, including *Sry* (Koopman et al., 1991), *Sox9* (Barrionuevo et al., 2006; Vidal et al., 2001), *Amh* (Behringer et al., 1994), *Dhh* (Yao et al., 2002), *Ptgds* (Adams and McLaren, 2002; Wilhelm et al., 2005), *Fgf9* (Bowles et al., 2010; Colvin et al., 2001) and *Cyp26b1* (cytochrome P450, family 26, subfamily b, polypeptide 1) (Bowles et al., 2006; Koubova et al., 2006) (Fig. 2 and Supplemental Fig. S2). We also detected many previously identified markers for testis differentiation, such as *Mmd2* (monocyte to macrophage differentiation associated 2) (Menke and Page, 2002), *Col9a3* (collagen, type IX, alpha 3), *Tesc* (tescalcin) (Perera et al., 2001), *Mro* (maestro) (Smith et al., 2003) and *Aldh1a1* (aldehyde dehydrogenase family 1, subfamily A1) (Bowles et al., 2009) (Supplemental Table S3). Interestingly, *Gm10352*, a predicted Y chromosomal gene located ~250 kb centromeric to *Sry*, exhibited an expression pattern similar to that of *Sry*, with a transient peak of expression at 11.5 dpc (Fig. 4). The similar expression profiles of these two neighboring genes suggests that they may be co-regulated by a common, possibly epigenetic mechanism (Kuroki et al., 2013; Kuroki et al., 2017), an intriguing possibility in light of the current lack of knowledge regarding *Sry* regulation (Larney et al., 2014).

At 12.5 and 13.5 dpc, the number of sex-biased genes in fetal testes and ovaries increased massively, reaching approximately 10% (2828) or 19% (5134) of all the expressed genes, respectively (Fig. 3A and Supplemental Table S3). This increase coincides with the differentiation and assembly of sex-specific cell lineages, and the rapid divergence in gonad morphology. Fetal testes undergo testis cord formation, vascularization and a substantial increase in volume (Svingen and Koopman, 2013) and, by 12.5 dpc, become easily

distinguishable from fetal ovaries which show no overt morphological changes (Fig. 1). Consistent with previous reports that sexual identity is established by 12.5 dpc in somatic cell lineages (Jameson et al., 2012b; Nef et al., 2005), we found that about 70% of the sex-biased genes at 12.5 dpc maintained their dimorphic expression at 13.5 dpc in both fetal testes and ovaries (Fig. 3B).

Pathway analysis of the sex-biased genes at 12.5 or 13.5 dpc revealed significant enrichment of genes associated with terms including organismal development, embryonic development, and reproductive system and function (Supplemental Table S3). Overrepresented molecular functions in the sex-biased genes include cell morphology, cellular growth and proliferation, cell death and survival, and lipid metabolism (Supplemental Table S3), providing molecular bases for the formation of sexually dimorphic morphology and the execution of sex-specific gonadal cell lineage differentiation programs.

We benchmarked our results against a dataset from the Capel group that is widely used in the field (Jameson et al., 2012b). Despite differences in experimental design (isolated cell populations *vs.* whole gonads), expression profiling technology (microarray *vs.* RNA-Seq), and analysis methods and statistical cut-offs, we found that ~50% of lineage-specific and sexually dimorphic genes at 12.5 and 13.5 dpc reported by Jameson et al. (Jameson et al., 2012b) were detected as sex-biased genes in the present study (Supplemental Fig. S3A). We also compared our data with a recently-published RNA-Seq dataset from 13.5-dpc fetal gonads (Rahmoun et al., 2017). Again, ~50% of genes reported as differentially expressed between wild type XX and XY fetal gonads at 13.5 dpc (Rahmoun et al., 2017) were detected as sex-biased in the present study (Supplemental Fig. S3B). The differences between the two

RNA-Seq datasets may be attributable, at least in part, to genetic background (Munger et al., 2009; Munger et al., 2013): inbred C57BL/6 mice (Rahmoun et al., 2017) *vs.* outbred Swiss albino (present study). Taken together, our data show a high degree of concordance with previous studies, but also uncover a large number of previously unidentified genes with sexually dimorphic expression during fetal gonadal differentiation.

3.3 Stage *vs.* stage comparison

We next sought to characterize the temporal dynamics of gene expression in mouse fetal gonads by comparing gene expression at one-day intervals in the developing testes or ovaries (Fig. 5A and Supplemental Table S4).

Between 10.5 and 11.5 dpc, 2129 genes were differentially expressed in XY genital ridges, while 2493 were differentially expressed in XX (Fig. 5A). The majority of those genes were up- or down-regulated similarly in XX and XY genital ridges over this period (Fig. 5B), consistent with the limited sexual dimorphic gene expression seen at 11.5 dpc (Fig. 3A). Among the 1230 commonly up-regulated genes were those important for genital ridge formation in both XX and XY embryos, such as *Gata4* (GATA binding protein 4) (Hu et al., 2013) and *Lhx9* (LIM homeobox 9) (Birk et al., 2000) (Fig. 5C). In addition, many germ cell-specific genes, including *Ddx4* (DEAD (Asp-Glu-Ala-Asp) box polypeptide 4), *Dazl* (deleted in azoospermia-like), *Nanog* (Nanog homeobox) and *Sox2* (SRY-box 2), were up-regulated during this period in both XX and XY genital ridges (Supplemental Table S4), as expected from the arrival and proliferation of germ cells, and their lack of sex differentiation, during this period (Spiller et al., 2017).

In the same time interval, 296 genes were down-regulated in both XX and XY genital ridges (Fig. 5B). The repression of at least some of those may be necessary to allow the formation and differentiation of genital ridges. For example, *Osr1* (odd-skipped related transcription factor 1) and *Pax2* (paired box 2) are expressed initially in the intermediate mesoderm giving rise to both kidneys and gonads, and their continued expression is consistent with their essential roles in kidney differentiation (James et al., 2006; Torres et al., 1995). Forced expression of *Pax2* in chicken genital ridges induces formation of ectopic nephric structures (Bouchard et al., 2002). Not surprisingly, expression of such genes is extinguished in gonads after 10.5 dpc, irrespective of sex (Fig. 5D).

From 11.5 to 12.5 dpc, 2893 and 1793 genes were differentially expressed in XX and XY gonads, respectively (Fig. 5A). In both sexes, more genes were down-regulated than up-regulated, suggesting that transcriptional repression may play important roles in early-stage gonadal differentiation (see below). Between 12.5 and 13.5 dpc, 831 and 1319 genes were differentially expressed in XX or XY gonads, respectively (Fig. 5A). From 11.5 to 13.5 dpc, the overlap of commonly regulated genes between XX and XY gonads decreased sharply (Fig. 5B), reflecting the engagement of sex-specific transcriptional programs during this period (Fig. 3A).

Notably, in the period 10.5–12.5 dpc, more temporally regulated genes were detected in XX than in XY gonads (Fig. 5A). Between 10.5 and 11.5 dpc, 967 genes changed expression levels in XX gonads only (583 up, 384 down), compared to 602 in XY only (470 up, 132

down; Fig. 5B). Between 11.5 to 12.5 dpc, 2047 genes changed expression levels in XX gonads only, compared to 950 in XY only (Fig. 5B and Supplemental Table S4). Taken together, these results support and extend previous observations (Nef et al., 2005) of an extensive ovary-specific transcriptional program in play right from the onset of fetal gonadal development.

We note that it is likely that the differential expression of a subset of identified down-regulated genes may be caused by the relative decrease in the proportion of cells expressing them in the developing gonads, especially from 12.5 to 13.5 dpc when various gonadal cell lineages undergo rapid proliferation resulting a significant change in cell proportion. Nevertheless, such genes do not seem to constitute a significant portion of the down-regulated genes, as the numbers of down-regulated genes identified in both XX and XY decreased substantially from 12.5 to 13.5 dpc, compared with those from 11.5 to 12.5 dpc (Fig. 5A).

3.4 Transcriptional activation *vs.* repression

Sexually dimorphic gene expression may be established by either transcriptional activation (up-regulation) or repression (down-regulation) in the developing fetal gonads. To examine the relative contribution of transcriptional activation and repression to the establishment of sexually dimorphic expression, we compared genes that acquired sex-biased expression with those regulated temporally during each 1-day interval from 10.5 to 13.5 dpc (Fig. 6).

Ninety-one genes acquired male-biased expression between 10.5 and 11.5 dpc (genes with male-biased expression in XY gonads at 11.5 dpc but not at 10.5 dpc). In the vast majority (81 of 91), this was caused by an up-regulation in XY, consistent with previous findings (Munger et al., 2013). Similarly, 6 of 9 genes acquired female-biased expression during this 1-day interval due to up-regulation in XX gonads. These results suggest that, at the onset of sex determination, sexually dimorphic gene expression is primarily established by transcriptional activation in each sex. Supporting this argument, we identified ~3-fold more up-regulated genes than down-regulated ones in both XX and XY genital ridges during the period 10.5–11.5 dpc (Fig. 5A).

The situation was very different between 11.5 and 12.5 dpc. In both XX and XY fetal gonads, genes having acquired sexually dimorphic expression now consisted of more genes down-regulated in the opposite sex than up-regulated in the relevant sex (Fig. 6), indicating a more prominent contribution of transcriptional repression to establishing the sexually dimorphic transcriptional program during this time. In line with this, more genes were down-regulated than up-regulated from 11.5 to 12.5 dpc in both XX and XY fetal gonads (Fig. 5A).

The trend reversed again during the interval 12.5 to 13.5 dpc. Genes having acquired sex-biased expression during this time included more genes up-regulated in the relevant sex than those down-regulated in the opposite sex (Fig. 6), likely reflecting, at least in part, the activation and advancement of lineage-specific transcriptional programs underpinning the differentiation of male interstitial and male/female germ cell lineages (Jameson et al., 2012b). As noted above, apparent down-regulation of gene expression may also be caused by a “dilution” effect due to rapidly changing cell proportion. Future studies using single-cell

RNA-Seq (Stévant et al., 2018) on various gonadal cell lineages are required to further address this issue.

3.5 Identification of co-expression modules

Co-expression of groups of genes normally reflects their close proximity within transcriptional networks (Babu et al., 2004; Stuart et al., 2003). To identify coordinately expressed gene modules that may be relevant to the control of sex determination and gonadal development, we performed a weighted gene co-expression network analysis (Langfelder and Horvath, 2008), an unbiased and unsupervised method to identify biologically meaningful transcriptional networks in the developing mouse gonads. Among 8966 genes included in this analysis, we identified 50 gene modules (Supplemental Fig. S4A) exhibiting distinct expression trajectories from 10.5 to 13.5 dpc. Twenty-one of the modules (dubbed A to U) showed significant positive or negative correlation with sex and/or developmental stage (Supplemental Fig. S4B and Supplemental Table S5).

Many of the sex- and/or stage-correlated modules were found to contain known sex determination and gonadal differentiation genes (Fig. 7 and Supplemental Table S5). As expected, pathway analysis of these modules revealed significant enrichment of genes involved in reproductive system development and function, embryonic development, organ/tissue morphology, and organ/tissue development (Supplemental Table S5).

Several modules contain genes highly expressed at 10.5 or 11.5 dpc but significantly down-regulated at later stages (Supplemental Fig. S4B). One such module (F) comprises genes that

were markedly up-regulated in both XX and XY genital ridges at 11.5 dpc, and then were gradually down-regulated in both sexes (Fig. 7). A notable module member, *Wt1* (Supplemental Table S5), is required for genital ridge formation in both XX and XY (Kreidberg et al., 1993). We speculate that other genes in this module may similarly be involved in the development of genital ridges in both sexes.

We identified 7 modules associated with testis development at 12.5 and/or 13.5 dpc (Supplemental Fig. S4B). Prominent among these are modules I and J, which contain known genes critical for Sertoli cell development and function (Fig. 7 and Supplemental Table S5), including *Sox9* (module I), *Amh, Fgf9, Aard* (alanine and arginine rich domain containing protein) and *Dhh* (module J). Module J appeared to be induced slightly later than module I (Fig. 7). In accordance with its timing of induction, module J includes many marker genes for testis differentiation, such as *Vnn1* (vanin 1), *Mro, Aldh1a1* and *Gstm6* (glutathione S-transferase, mu 6) (Supplemental Table S5). The two modules are enriched for genes involved in cellular growth and proliferation, cell cycle, cell-to-cell signaling and interaction, and cellular assembly and organization (Supplemental Table S5), molecular functions likely underpinning the rapid proliferation and coordinated differentiation, migration and assembly of testicular cell lineages in XY gonads in the period 12.5–13.5 dpc (Svingen and Koopman, 2013; Ungewitter and Yao, 2013).

Conversely, 8 modules were strongly activated during ovarian development (Supplemental Fig. S4B and Supplemental Table S5); these included modules N and S (Fig. 7). These two modules contain genes critically involved in WNT signaling (module N: *Rspo1*, *Wnt4* and *Lef1* (lymphoid enhancer binding factor 1)), female somatic cell lineage differentiation

(module N: *Bmp2* and *Nr0b1* (nuclear receptor subfamily 0, group B, member 1; also known as *Dax1*); module S: *Foxl2* and *Fst*), and germ cell entry of meiosis (module S: *Stra8*, *Sycp3* (synaptonemal complex protein 3) and *Dmc1*) (Supplemental Table S5).

As expected, some modules that positively correlated with one sexual fate show concomitant negative correlations with the alternative fate. For example, modules I and O were significantly repressed in XX or XY gonads, respectively (Fig. 7 and Supplemental Fig. S4B), reinforcing the concept that normal development in each sex relies in part on repression of the regulatory networks underpinning development in the opposite sex.

3.6 Alternative splicing

An important advantage of RNA-Seq technology is that it allows transcript isoforms to be distinguished and quantitated in an unbiased, genome-wide manner. To this end, we mapped sequencing reads to all annotated transcripts in Ensembl 75 reference transcriptome using the RSEM algorithm (Li and Dewey, 2011), which uses a maximization of expectation approach to assign reads to transcript isoforms (Li et al., 2010) and outputs the relative abundance (isoform percentage) and expression level (TPM) of each isoform. Differential expression analysis at the transcript level was performed using edgeR (Robinson et al., 2010), similar to the gene-level analysis described above. Since the distribution of reads among isoforms expressed at very low levels may not be accurate (Zhao et al., 2015), we removed transcripts expressed at very low levels using a cut-off of TPM > 5 and isoform percentage > 10% in sample 11.5M2 or at least two other samples.

We detected in total 19,449 transcripts, representing 12,276 genes, expressed above the defined threshold in the developing mouse gonads (Fig. 8A and Supplemental Table S6). Over 36% of the genes (4477) expressed multiple transcript isoforms during the time course (Fig. 8A and Supplemental Table S6), indicating widespread alternative splicing in mouse fetal gonads. Among the expressed transcripts, hundreds of them were differentially expressed in a sex- or stage-dependent manner, thus providing a picture of transcriptional regulation at the transcript isoform level (Supplemental Fig. S5 and Supplemental Table S6). Validating this approach, we identified four different transcript forms of *Wt1*, including those encoding the well-characterized +KTS and –KTS protein isoforms known to play important but distinct roles in sex determination and gonadal development (Hammes et al., 2001).

3.7 Regulation of splicing in the developing fetal gonads

Having identified genes that are alternative spliced in the fetal gonads, i.e. those expressing multiple transcript isoforms, we next sought to determine whether and how the splicing of these genes is regulated. To this end we sought to identify genes that were differentially spliced between sexes or stages, namely, genes that express different isoforms or express the same set of isoforms but with different levels of representation in the different samples being compared.

We used an exon-centric approach to identify genome-wide differentially spliced exonic regions between two sexes or two consecutive time points using the DEXSeq package (Anders et al., 2012). DEXSeq calculates the exon usage defined as the ratio of reads mapped to a particular exonic region and those mapped to all other exonic regions of the same gene,

and tests whether the exon usage differs significantly between conditions using a generalized linear model, thereby providing information of differential splicing at the exon level. The identified differentially spliced exonic regions were then mapped to gene models to determine genes that were differentially spliced in a sex- or stage-dependent manner. We refer to such genes as differentially spliced genes (DSGs),

We first analyzed sex-dependent regulation of splicing events by comparing the usage of all annotated exonic regions between XX and XY at each time point. No differentially spliced exonic regions were identified at 10.5 dpc with a cut-off of adjusted *P* value of 0.05 and $\log_2$ fold change of 1 (Fig. 8B), consistent with the bi-potential nature of genital ridges at this stage. Accompanying the establishment of sexually dimorphic gene expression, we identified 14 exonic regions (corresponding to 12 genes) differentially spliced between the sexes at 11.5 dpc, 244 (110 genes) at 12.5 dpc, and 285 (173 genes) at 13.5 dpc (Fig. 8B, Supplemental Fig. S6A, and Supplemental Table S7). Most of the sex-biased splicing events appear to be stage-dependent during this time window, as there is limited overlap of differentially spliced exons or genes between the time points studied from 11.5 to 13.5 dpc (Fig. 8C and Supplemental Fig. S6B). Validating our analysis, *Fgfr2* (fibroblast growth factor receptor 2) was found to exhibit sex-biased alternative splicing, with increased inclusion of exon 9 encoding the FGFR2c isoform in XX fetal gonads at 12.5 dpc (Supplemental Fig. S7 and Supplemental Table S7), consistent with a recent report (Rahmoun et al., 2017).

We next analyzed temporal regulation of alternative splicing and identified large numbers of exonic regions differentially spliced between two stages in XX or XY fetal gonads (Fig. 8D, Supplemental Fig. S6C, and Supplemental Table S7). Notably, the dynamics of temporally

regulated splicing exons/genes differed between the two sexes (Fig. 8D and Supplemental Fig. S6C): In XY fetal gonads, the largest number of temporally regulated splicing events was found between 10.5 and 11.5 dpc, and the numbers decreased sharply afterwards. In contrast, the number of temporally regulated splicing events peaked between 11.5 and 12.5 dpc in XX fetal gonads.

We further compared genes differentially spliced between the two sexes with those with sexually dimorphic expression, and found that over 40% of differentially spliced genes were also differentially expressed between XX and XY at 12.5 and 13.5 dpc (Supplemental Fig. S8)—that is, these genes were regulated at both the RNA transcription and splicing levels to establish sexual dimorphism.

Notably, *Wt1* was not identified as a DSG in the DEXSeq analysis, suggesting that splicing of *Wt1* was not regulated in a sex- or stage-dependent manner in mouse fetal gonads. To understand regulation of splicing in mouse fetal gonadal development at a global level, we compared DSGs to those alternative spliced genes in mouse fetal gonads. Of all RSEM-identified alternatively spliced genes (defined as those expressing multiple major transcript isoforms) in mouse fetal gonads (4477 genes, Supplemental Table S6), only a small proportion (808 genes, 18%; Supplemental Fig. S9) was differentially spliced in an either sex-biased or temporally-regulated manner (Supplemental Table S7). This suggests that splicing of the majority of genes expressing multiple transcript isoforms in mouse fetal gonads was independent of the sex or stage.

3.8 Spatio-temporal regulation of *Lef1* splicing in mouse fetal gonads

Given the known roles that alternative splicing plays in the development of other organs (Baralle and Giudice, 2017), we considered it likely that the spatio-temporal regulation of alternative splicing may also have functional implications in fetal gonadal development. Supporting this concept, we found that many of the identified differentially spliced genes (DSGs), when mutated in mice, can result in various phenotypes of the reproductive system including abnormal morphology and infertility (Mouse Genome Informatics database; Supplemental Table S7), implicating that sex-biased and/or temporally-regulated differential splicing of these genes in the developing fetal gonads may play yet-to-be identified roles in regulating the differentiation and development of the reproductive system.

We next focused on *Lef1*, the splicing of which was shown to be regulated in a sex- and stage-dependent manner in mouse fetal gonads. LEF1 is a key mediator of the canonical WNT signaling pathway, which plays a critical role in driving ovarian development (Chassot et al., 2008; Liu et al., 2009; Parma et al., 2006; Vainio et al., 1999) and also influences testis development (Jeays-Ward et al., 2004). Regulation of splicing of *Lef1* (and *Tcf7l2* (transcription factor 7 like 2, T cell specific, HMG box; also known as *Tcf4*)) has been recognized as an important way to regulate WNT signaling pathway activity (Arce et al., 2006; Hoppler and Kavanagh, 2007).

Our results revealed that the inclusion of *Lef1* exon 6 was significantly increased in XX genital ridges from 10.5 to 11.5 dpc (top right circle, Fig. 9A; Supplemental Table S7). The increase appeared to have continued between 11.5 and 12.5 dpc in XX gonads (P = 0.003),

but just fell short of the $\log_2$ fold change cutoff of 1 (0.973; central right circle, Fig. 9A). This splicing pattern was maintained in XX gonads from 12.5 to 13.5 dpc. In contrast, no significant difference in exon 6 usage was detected in XY fetal gonads during the entire time course (squares, Fig. 9A). As a result, we identified significantly higher levels of exon 6 inclusion in XX gonads than XY at 12.5 and 13.5 dpc (diamonds, Fig. 9A; Fig. 9B,C and Supplemental Table S7).

The 83-nucleotide exon 6 encodes part of the context-dependent regulatory domain, which has been shown to be important for LEF1 to activate its target genes (Gradl et al., 2002; Mallory et al., 2011). The skipping of exon 6 leads to the generation of a smaller LEF1* protein, which is less potent than the exon 6-included full-length protein in activating target enhancers in transfection assays (Carlsson et al., 1993). The increased inclusion of exon 6 in *Lef1* mRNA in XX gonads between 10.5 and 12.5 dpc presumably led to the generation of more full-length LEF1 protein at the expense of exon 6-skipped LEF1*. Notably, female-biased expression of *Lef1* was also established by 12.5 dpc (Fig. 9D). As a result of combined regulation at both the transcriptional and RNA-splicing level, more full-length LEF1 protein possessing higher transactivation capacity is predicted to be produced in XX gonads, ensuring the successful transduction of WNT signaling to secure fetal ovarian development.

4. DISCUSSION

In the present study, we have used RNA-Seq to characterize the sexually dimorphic transcriptional program in mouse fetal gonads at four key developmental stages, in order to provide insights into the regulation of sex determination and gonadal development. While several previous studies have addressed this question (Beverdam and Koopman, 2006; Bouma et al., 2007; Bouma et al., 2010; Jameson et al., 2012b; Munger et al., 2013; Nef et al., 2005; Small et al., 2005), ours is the first to combine the technological advantages of RNA-Seq, a time-course of successive developmental stages, and a scope of analysis that is not limited to one cell lineage. Our results provide a resource for continued studies in the areas of sex determination, testis and ovary differentiation, and germ cell development, and reveal a complex landscape of transcriptional activation, repression and alternative splicing at play in these systems.

4.1 A transcriptional map of gonadal development

Our data reaffirm previous findings (Beverdam and Koopman, 2006; Jameson et al., 2012b; Nef et al., 2005) that organogenesis of the testes and ovaries involves complex transcriptional networks that, as in other developing organs, orchestrate cell proliferation, migration, differentiation, interaction and function. Within these networks, genes are both activated and repressed. Extending previous observations that a female-specific transcriptional program initiates at 11.5 dpc and rapidly expands from 11.5 to 13.5 dpc (Beverdam and Koopman, 2006; Jameson et al., 2012b; Nef et al., 2005), we have found that a large number of genes were already exclusively up- or down-regulated in XX genital ridges between 10.5 and 11.5 dpc, before overt sexually dimorphic gene expression (and morphological differences) is established. These findings indicate that in XX embryos, the ovarian differentiation program

has already started despite the genital ridges remaining morphologically indifferent and sexually bipotent at this stage.

The relative contributions of transcriptional activation and repression to establishing sexually dimorphic gene expression were surprisingly fluid. In general, activation events outweighed repression events, but, surprisingly, between 11.5 and 12.5 dpc, the reverse was true. This transient surge in the relative contribution of transcriptional repression to sex-biased gene expression took place immediately after sex determination but before overt morphological differences appeared. The timing of the shift points to a potential role of transcriptional repression in canalizing gonad development along the male or female pathway, reinforcing the concept of mutual antagonism between the testis- and ovary-specific pathways (Bagheri-Fam et al., 2017; Chang et al., 2008; Greenfield, 2015; Jameson et al., 2012a; Kashimada et al., 2011; Kim et al., 2006; Maatouk et al., 2008; Wilhelm et al., 2009).

We have included duplicate tissue pools for most conditions in the RNA-Seq analysis, mainly due to the limited material available, especially at 10.5 and 11.5 dpc. To mitigate the statistical concerns, each tissue pool contained gonadal tissue from multiple embryos (>20 at 10.5/11.5 dpc; >3 at 12.5/13.5 dpc) and the analysis was performed using edgeR, which is specially designed to accommodate situates where limited numbers of biological replicates are available (McCarthy et al., 2012). Supporting these, we showed that expression profiles of almost all known sex marker genes in our RNA-Seq data are consistent with their documented expression patterns. In addition, our dataset shows a high concordance with other published expression profiling datasets.

4.2 Alternative splicing

Alternative splicing allows the generation of multiple transcript isoforms from a single gene; these isoforms may exhibit differences in mRNA stability, localization, or translation, and may generate diverse protein products. It plays important roles in the development of various organs, including the brain, heart and liver, where it influences cell lineage determination and differentiation, and tissue-identity acquisition and maintenance (Baralle and Giudice, 2017). Intriguingly, alternative splicing plays a central role in insect sex determination (Bopp et al., 2014) and has been recently implicated in reptile temperature-dependent sex determination (Deveson et al., 2017).

An important feature of RNA-Seq technology is that it provides a window to the spliceome. Using RNA-Seq, we detected widespread alternative splicing in fetal gonadal development. For example, we identified four abundantly expressed mRNA isoforms of *Wt1*, including those encoding the well-established +/–KTS protein isoforms (Hammes et al., 2001).

The majority of genes expressing multiple transcript isoforms in mouse fetal gonads, including *Wt1*, however, was not differentially spliced, indicating that their splicing was independent of the sex or stage. We then focused on genes that are differentially spliced between sexes and stages during mouse fetal gonadal development, as this information may offer novel insights into how gonadogenesis is regulated at the transcriptional level.

Supporting our hypothesis that the splicing regulation of the identified DSGs may have important functions in gonadal development, many identified DSGs have been associated with reproductive phenotypes when mutated in mice. Nevertheless, the exact molecular consequences of the differential splicing events, in most cases, are difficult to predict, primarily due to the very limited information of protein structure-function relations available for the majority of the identified DSGs. Furthermore, many of the associated reproductive phenotypes appear to be related to developmental abnormalities of the germ cell lineage, and it is not clear at present whether differential splicing of these genes may contribute to the regulation of somatic sex development. Nevertheless, our data should provide some leads for future work.

Notably, we found that splicing of *Lef1* exon 6 was tightly regulated in a sex- and stage-dependent manner. In combination with up-regulated expression of *Lef1* in fetal ovaries, the female-biased regulation of *Lef1* splicing should lead to the generation of larger amount of exon 6-included full-length LEF1 possessing a more potent transactivation capacity in XX gonads at the right time, thereby ensuring a coordinated enhancement of WNT signaling activity to secure fetal ovarian development.

Regulation of *Lef1* exon 6 splicing was previously reported in postnatal mouse brain development (Nagalski et al., 2013) and T-cell activation (Mallory et al., 2011). In the latter case, a RNA-binding protein CELF2 (CUGBP Elav-like family member 2) has been shown to bind to the flanking intronic sequences and regulate exon 6 splicing (Mallory et al., 2011). However, CELF2 seems unlikely to regulate the female-specific inclusion of *Lef1* exon 6, since it was expressed at similar levels in XX and XY gonads during the entire time course

(Supplemental Table S2), suggesting other unidentified factors at play. In this regard, we note several splicing factors manifesting sexually dimorphic expression in fetal gonads, including *Sf3b4* (splicing factor 3b, subunit 4), *Esrp1* (epithelial splicing regulatory protein 1), and *Srsf12* (serine and arginine rich splicing factor 12) (Supplemental Table S3).

Given our finding of widespread stage- and sex-specific regulation of transcript isoform usage in the fetal gonads, and the implication that this may represent an important additional layer in the regulation of mammalian sex determination and/or gonadal development, it would be of interest to use RNA-Seq to investigate the lineage specificity of this phenomenon. This was not done in the present study as we lacked the appropriate suite of reporter strains described by Jameson et al. (2012b), but would be a useful goal for future investigations.

In summary, the RNA-seq dataset described here provides a new level of detail concerning the transcriptional landscape in the developing mouse fetal gonads, including sex-specific and temporal changes not only in gene or transcript expression, but also in mRNA splicing. We envisage that this dataset will prove a useful resource for the field to decipher the transcriptional control mechanisms underpinning mammalian sex determination and fetal gonadal differentiation, and to identify promising candidate genes involved in human DSDs.

Acknowledgements

This work was supported by the National Health and Medical Research Council (NHMRC) of Australia and the Australian Research Council. PK is a Senior Principal Research Fellow of the NHMRC. CMS is a University of Queensland Postdoctoral Research Fellow. We thank Tara-Lynne Davidson for assistance with mouse husbandry, and Drs Nadia Davidson and Alicia Oshlack (Murdoch Children's Research Institute, Melbourne, Australia) for preliminary data analysis.

REFERENCES

Adams, I.R., McLaren, A., 2002. Sexually dimorphic development of mouse primordial germ cells: switching from oogenesis to spermatogenesis. Development. 129, 1155-1164.

Anders, S., Reyes, A., Huber, W., 2012. Detecting differential usage of exons from RNA-seq data. Genome Res. 22, 2008-2017.

Arce, L., Yokoyama, N.N., Waterman, M.L., 2006. Diversity of LEF/TCF action in development and disease. Oncogene. 25, 7492-7504.

Babu, M.M., Luscombe, N.M., Aravind, L., Gerstein, M., Teichmann, S.A., 2004. Structure and evolution of transcriptional regulatory networks. Curr. Opin. Struct. Biol. 14, 283-291.

Bagheri-Fam, S., Bird, A.D., Zhao, L., Ryan, J.M., Yong, M., Wilhelm, D., Koopman, P., Eswarakumar, J.V., Harley, V.R., 2017. Testis determination requires a specific FGFR2 isoform to repress FOXL2. Endocrinology. 158, 3832-3843.

Baker, P.J., Sha, J.A., McBride, M.W., Peng, L., Payne, A.H., O'Shaughnessy, P.J., 1999. Expression of 3beta-hydroxysteroid dehydrogenase type I and type VI isoforms in the mouse testis during development. Eur. J. Biochem. 260, 911-917.

Baralle, F.E., Giudice, J., 2017. Alternative splicing as a regulator of development and tissue identity. Nat. Rev. Mol. Cell Biol. 18, 437-451.

Barrionuevo, F., Bagheri-Fam, S., Klattig, J.r., Kist, R., Taketo, M.M., Englert, C., Scherer, G., 2006. Homozygous Inactivation of Sox9 Causes Complete XY Sex Reversal in Mice. Biol. Reprod. 74, 195-201.

Behringer, R.R., Finegold, M.J., Cate, R.L., 1994. Müllerian-inhibiting substance function during mammalian sexual development. Cell. 79, 415-425.

Beverdam, A., Koopman, P., 2006. Expression profiling of purified mouse gonadal somatic cells during the critical time window of sex determination reveals novel candidate genes for human sexual dysgenesis syndromes. Hum. Mol. Genet. 15, 417-431.

Birk, O.S., Casiano, D.E., Wassif, C.A., Cogliati, T., Zhao, L., Zhao, Y., Grinberg, A., Huang, S., Kreidberg, J.A., Parker, K.L., Porter, F.D., Westphal, H., 2000. The LIM homeobox gene Lhx9 is essential for mouse gonad formation. Nature. 403, 909-913.

Bitgood, M.J., Shen, L., McMahon, A.P., 1996. Sertoli cell signaling by Desert hedgehog regulates the male germline. Curr. Biol. 6, 298-304.

Bolger, A.M., Lohse, M., Usadel, B., 2014. Trimmomatic: a flexible trimmer for Illumina sequence data. Bioinformatics. 30, 2114-2120.

Bopp, D., Saccone, G., Beye, M., 2014. Sex Determination in Insects: Variations on a Common Theme. Sex. Dev. 8, 20-28.

Bouchard, M., Souabni, A., Mandler, M., Neubuser, A., Busslinger, M., 2002. Nephric lineage specification by Pax2 and Pax8. Genes Dev. 16, 2958-2970.

Bouma, G.J., Affourtit, J.P., Bult, C.J., Eicher, E.M., 2007. Transcriptional profile of mouse pre-granulosa and Sertoli cells isolated from early-differentiated fetal gonads. Gene Expr. Patterns. 7, 113-123.

Bouma, G.J., Hudson, Q.J., Washburn, L.L., Eicher, E.M., 2010. New Candidate Genes Identified for Controlling Mouse Gonadal Sex Determination and the Early Stages of Granulosa and Sertoli Cell Differentiation. Biol. Reprod. 82, 380-389.

Bowles, J., Feng, C.-W., Knight, D., Smith, C.A., Roeszler, K.N., Bagheri-Fam, S., Harley, V.R., Sinclair, A.H., Koopman, P., 2009. Male-specific expression of Aldh1a1 in mouse and chicken fetal testes: Implications for retinoid balance in gonad development. Dev. Dyn. 238, 2073-2080.

Bowles, J., Feng, C.W., Spiller, C., Davidson, T.L., Jackson, A., Koopman, P., 2010. FGF9 suppresses meiosis and promotes male germ cell fate in mice. Dev. Cell. 19, 440-449.

Bowles, J., Knight, D., Smith, C., Wilhelm, D., Richman, J., Mamiya, S., Yashiro, K., Chawengsaksophak, K., Wilson, M.J., Rossant, J., Hamada, H., Koopman, P., 2006. Retinoid signaling determines germ cell fate in mice. Science. 312, 596-600.

Brown, C.J., Ballabio, A., Rupert, J.L., Lafreniere, R.G., Grompe, M., Tonlorenzi, R., Willard, H.F., 1991. A gene from the region of the human X inactivation centre is expressed exclusively from the inactive X chromosome. Nature. 349, 38-44.

Bullejos, M., Koopman, P., 2001. Spatially dynamic expression of Sry in mouse genital ridges. Dev. Dyn. 221, 201-205.

Carlsson, P., Waterman, M.L., Jones, K.A., 1993. The hLEF/TCF-1 alpha HMG protein contains a context-dependent transcriptional activation domain that induces the TCR alpha enhancer in T cells. Genes Dev. 7, 2418-2430.

Chang, H., Gao, F., Guillou, F., Taketo, M.M., Huff, V., Behringer, R.R., 2008. Wt1 negatively regulates beta-catenin signaling during testis development. Development. 135, 1875-1885.

Chassot, A.-A., Ranc, F., Gregoire, E.P., Roepers-Gajadien, H.L., Taketo, M.M., Camerino, G., de Rooij, D.G., Schedl, A., Chaboissier, M.-C., 2008. Activation of β-catenin signaling by Rspo1 controls differentiation of the mammalian ovary. Hum. Mol. Genet. 17, 1264-1277.

Colvin, J.S., Green, R.P., Schmahl, J., Capel, B., Ornitz, D.M., 2001. Male-to-Female Sex Reversal in Mice Lacking Fibroblast Growth Factor 9. Cell. 104, 875-889.

da Silva, S.M., Hacker, A., Harley, V., Goodfellow, P., Swain, A., Lovell-Badge, R., 1996. Sox9 expression during gonadal development implies a conserved role for the gene in testis differentiation in mammals and birds. Nat. Genet. 14, 62-68.

Del Valle, I., Buonocore, F., Duncan, A.J., Lin, L., Barenco, M., Parnaik, R., Shah, S., Hubank, M., Gerrelli, D., Achermann, J.C., 2017. A genomic atlas of human adrenal and gonad development. Wellcome Open Res. 2, 25.

Deveson, I.W., Holleley, C.E., Blackburn, J., Marshall Graves, J.A., Mattick, J.S., Waters, P.D., Georges, A., 2017. Differential intron retention in Jumonji chromatin modifier genes is implicated in reptile temperature-dependent sex determination. Sci. Adv. 3, e1700731.

Dobin, A., Davis, C.A., Schlesinger, F., Drenkow, J., Zaleski, C., Jha, S., Batut, P., Chaisson, M., Gingeras, T.R., 2013. STAR: ultrafast universal RNA-seq aligner. Bioinformatics. 29, 15-21.

Eggers, S., Sadedin, S., van den Bergen, J.A., Robevska, G., Ohnesorg, T., Hewitt, J., Lambeth, L., Bouty, A., Knarston, I.M., Tan, T.Y., Cameron, F., Werther, G., Hutson, J., O'Connell, M., Grover, S.R., Heloury, Y., Zacharin, M., Bergman, P., Kimber, C., Brown, J., Webb, N., Hunter, M.F., Srinivasan, S., Titmuss, A., Verge, C.F., Mowat, D., Smith, G., Smith, J., Ewans, L., Shalhoub, C., Crock, P., Cowell, C., Leong, G.M., Ono, M., Lafferty, A.R., Huynh, T., Visser, U., Choong, C.S., McKenzie, F., Pachter, N., Thompson, E.M., Couper, J., Baxendale, A., Gecz, J., Wheeler, B.J., Jefferies, C., MacKenzie, K., Hofman, P., Carter, P., King, R.I., Krausz, C., van Ravenswaaij-Arts, C.M.A., Looijenga, L., Drop, S., Riedl, S., Cools, M., Dawson, A., Juniarto, A.Z., Khadilkar, V., Khadilkar, A., Bhatia, V., Dũng, V.C., Atta, I., Raza, J., thi Diem Chi, N.,

Hao, T.K., Harley, V., Koopman, P., Warne, G., Faradz, S., Oshlack, A., Ayers, K.L., Sinclair, A.H., 2016. Disorders of sex development: insights from targeted gene sequencing of a large international patient cohort. Genome Biol. 17, 243.

Gradl, D., Konig, A., Wedlich, D., 2002. Functional diversity of Xenopus lymphoid enhancer factor/T-cell factor transcription factors relies on combinations of activating and repressing elements. J. Biol. Chem. 277, 14159-14171.

Greenfield, A., 2015. Understanding sex determination in the mouse: genetics, epigenetics and the story of mutual antagonisms. J. Genet. 94, 585-590.

Hacker, A., Capel, B., Goodfellow, P., Lovell-Badge, R., 1995. Expression of Sry, the mouse sex determining gene. Development. 121, 1603-1614.

Hadjantonakis, A.-K., Gertsenstein, M., Ikawa, M., Okabe, M., Nagy, A., 1998. Non-invasive sexing of preimplantation stage mammalian embryos. Nat. Genet. 19, 220-222.

Hammes, A., Guo, J.-K., Lutsch, G., Leheste, J.-R., Landrock, D., Ziegler, U., Gubler, M.-C., Schedl, A., 2001. Two Splice Variants of the Wilms' Tumor 1 Gene Have Distinct Functions during Sex Determination and Nephron Formation. Cell. 106, 319-329.

Haque, A., Engel, J., Teichmann, S.A., Lonnberg, T., 2017. A practical guide to single-cell RNA-sequencing for biomedical research and clinical applications. Genome Med. 9, 75.

Hoppler, S., Kavanagh, C.L., 2007. Wnt signalling: variety at the core. J. Cell Sci. 120, 385-393.

Houmard, B., Small, C., Yang, L., Naluai-Cecchini, T., Cheng, E., Hassold, T., Griswold, M., 2009. Global Gene Expression in the Human Fetal Testis and Ovary. Biol. Reprod. 81, 438-443.

Hu, Y.-C., Okumura, L.M., Page, D.C., 2013. Gata4 Is Required for Formation of the Genital Ridge in Mice. PLoS Genet. 9, e1003629.

Hulsen, T., de Vlieg, J., Alkema, W., 2008. BioVenn – a web application for the comparison and visualization of biological lists using area-proportional Venn diagrams. BMC Genomics. 9, 488.

Ikeda, Y., Shen, W.H., Ingraham, H.A., Parker, K.L., 1994. Developmental expression of mouse steroidogenic factor-1, an essential regulator of the steroid hydroxylases. Mol. Endocrinol. 8, 654-662.

Inoue, M., Shima, Y., Miyabayashi, K., Tokunaga, K., Sato, T., Baba, T., Ohkawa, Y., Akiyama, H., Suyama, M., Morohashi, K., 2016. Isolation and Characterization of Fetal Leydig Progenitor Cells of Male Mice. Endocrinology. 157, 1222-1233.

James, R.G., Kamei, C.N., Wang, Q., Jiang, R., Schultheiss, T.M., 2006. Odd-skipped related 1 is required for development of the metanephric kidney and regulates formation and differentiation of kidney precursor cells. Development. 133, 2995-3004.

Jameson, S.A., Lin, Y.-T., Capel, B., 2012a. Testis development requires the repression of Wnt4 by Fgf signaling. Dev. Biol. 370, 24-32.

Jameson, S.A., Natarajan, A., Cool, J., DeFalco, T., Maatouk, D.M., Mork, L., Munger, S.C., Capel, B., 2012b. Temporal transcriptional profiling of somatic and germ cells reveals biased lineage priming of sexual fate in the fetal mouse gonad. PLoS Genet. 8, e1002575.

Jeays-Ward, K., Dandonneau, M., Swain, A., 2004. Wnt4 is required for proper male as well as female sexual development. Dev. Biol. 276, 431-440.

Jeske, Y.W., Mishina, Y., Cohen, D.R., Behringer, R.R., Koopman, P., 1996. Analysis of the role of Amh and Fra1 in the Sry regulatory pathway. Mol. Reprod. Dev. 44, 153-158.

Jorgensen, J.S., Gao, L., 2005. Irx3 is differentially up-regulated in female gonads during sex determination. Gene Expr. Patterns. 5, 756-762.

Kashimada, K., Svingen, T., Feng, C.-W., Pelosi, E., Bagheri-Fam, S., Harley, V.R., Schlessinger, D., Bowles, J., Koopman, P., 2011. Antagonistic regulation of Cyp26b1 by transcription factors SOX9/SF1 and FOXL2 during gonadal development in mice. FASEB J. 25, 3561-3569.

Kent, J., Wheatley, S.C., Andrews, J.E., Sinclair, A.H., Koopman, P., 1996. A male-specific role for SOX9 in vertebrate sex determination. Development. 122, 2813-2822.

Kim, Y., Kobayashi, A., Sekido, R., DiNapoli, L., Brennan, J., Chaboissier, M.-C., Poulat, F., Behringer, R.R., Lovell-Badge, R., Capel, B., 2006. Fgf9 and Wnt4 Act as Antagonistic Signals to Regulate Mammalian Sex Determination. PLoS Biol. 4, e187.

Koopman, P., Gubbay, J., Vivian, N., Goodfellow, P., Lovell-Badge, R., 1991. Male development of chromosomally female mice transgenic for Sry. Nature. 351, 117-121.

Koopman, P., Munsterberg, A., Capel, B., Vivian, N., Lovell-Badge, R., 1990. Expression of a candidate sex-determining gene during mouse testis differentiation. Nature. 348, 450-452.

Koubova, J., Menke, D.B., Zhou, Q., Capel, B., Griswold, M.D., Page, D.C., 2006. Retinoic acid regulates sex-specific timing of meiotic initiation in mice. Proc. Natl. Acad. Sci. USA. 103, 2474-2479.

Kreidberg, J.A., Sariola, H., Loring, J.M., Maeda, M., Pelletier, J., Housman, D., Jaenisch, R., 1993. WT-1 is required for early kidney development. Cell. 74, 679-691.

Kuroki, S., Matoba, S., Akiyoshi, M., Matsumura, Y., Miyachi, H., Mise, N., Abe, K., Ogura, A., Wilhelm, D., Koopman, P., Nozaki, M., Kanai, Y., Shinkai, Y., Tachibana, M., 2013. Epigenetic Regulation of Mouse Sex Determination by the Histone Demethylase Jmjd1a. Science. 341, 1106-1109.

Kuroki, S., Okashita, N., Baba, S., Maeda, R., Miyawaki, S., Yano, M., Yamaguchi, M., Kitano, S., Miyachi, H., Itoh, A., Yoshida, M., Tachibana, M., 2017. Rescuing the aberrant sex development of H3K9 demethylase Jmjd1a-deficient mice by modulating H3K9 methylation balance. Plos Genet. 13, e1007034.

Langfelder, P., Horvath, S., 2008. WGCNA: an R package for weighted correlation network analysis. BMC Bioinformatics. 9, 559.

Larney, C., Bailey, T.L., Koopman, P., 2014. Switching on sex: transcriptional regulation of the testis-determining gene Sry. Development. 141, 2195-2205.

Le Bouffant, R., Souquet, B., Duval, N., Duquenne, C., Hervé, R., Frydman, N., Robert, B., Habert, R., Livera, G., 2011. Msx1 and Msx2 promote meiosis initiation. Development. 138, 5393-5402.

Li, B., Dewey, C., 2011. RSEM: accurate transcript quantification from RNA-Seq data with or without a reference genome. BMC Bioinformatics. 12, 323.

Li, B., Ruotti, V., Stewart, R.M., Thomson, J.A., Dewey, C.N., 2010. RNA-Seq gene expression estimation with read mapping uncertainty. Bioinformatics. 26, 493-500.

Li, Y., Zheng, M., Lau, Y.-Fai C., 2014. The sex-determining factors SRY and SOX9 regulate similar target genes and promote testis cord formation during testicular differentiation. Cell Rep. 8, 723-733.

Liu, C.F., Bingham, N., Parker, K., Yao, H.H.C., 2009. Sex-specific roles of β-catenin in mouse gonadal development. Hum. Mol. Genet. 18, 405-417.

Loffler, K.A., Zarkower, D., Koopman, P., 2003. Etiology of ovarian failure in blepharophimosis ptosis epicanthus inversus syndrome: FOXL2 is a conserved, early-acting gene in vertebrate ovarian development. Endocrinology. 144, 3237-3243.

Maatouk, D.M., DiNapoli, L., Alvers, A., Parker, K.L., Taketo, M.M., Capel, B., 2008. Stabilization of β-catenin in XY gonads causes male-to-female sex-reversal. Hum. Mol. Genet. 17, 2949-2955.

Mallory, M.J., Jackson, J., Weber, B., Chi, A., Heyd, F., Lynch, K.W., 2011. Signal- and Development-Dependent Alternative Splicing of LEF1 in T Cells Is Controlled by CELF2. Mol. Cell. Biol. 31, 2184-2195.

McCarthy, D.J., Chen, Y., Smyth, G.K., 2012. Differential expression analysis of multifactor RNA-Seq experiments with respect to biological variation. Nucleic Acids Res. 40, 4288-4297.

McClelland, K.S., Bell, K., Larney, C., Harley, V.R., Sinclair, A.H., Oshlack, A., Koopman, P., Bowles, J., 2015. Purification and transcriptomic analysis of mouse fetal leydig cells reveals candidate genes for specification of gonadal steroidogenic cells. Biol. Reprod. 92, 145.

Menke, D.B., Koubova, J., Page, D.C., 2003. Sexual differentiation of germ cells in XX mouse gonads occurs in an anterior-to-posterior wave. Dev. Biol. 262, 303-312.

Menke, D.B., Page, D.C., 2002. Sexually dimorphic gene expression in the developing mouse gonad. Gene Expr. Patterns. 2, 359-367.

Munger, S.C., Aylor, D.L., Syed, H.A., Magwene, P.M., Threadgill, D.W., Capel, B., 2009. Elucidation of the transcription network governing mammalian sex determination by exploiting strain-specific susceptibility to sex reversal. Genes Dev. 23, 2521-2536.

Munger, S.C., Natarajan, A., Looger, L.L., Ohler, U., Capel, B., 2013. Fine Time Course Expression Analysis Identifies Cascades of Activation and Repression and Maps a Putative Regulator of Mammalian Sex Determination. PLoS Genet. 9, e1003630.

Munsterberg, A., Lovell-Badge, R., 1991. Expression of the mouse anti-mullerian hormone gene suggests a role in both male and female sexual differentiation. Development. 113, 613-624.

Nagalski, A., Irimia, M., Szewczyk, L., Ferran, J.L., Misztal, K., Kuznicki, J., Wisniewska, M.B., 2013. Postnatal isoform switch and protein localization of LEF1 and TCF7L2

transcription factors in cortical, thalamic, and mesencephalic regions of the adult mouse brain. Brain Struct. Funct. 218, 1531-1549.

Nef, S., Schaad, O., Stallings, N.R., Cederroth, C.R., Pitetti, J.-L., Schaer, G., Malki, S., Dubois-Dauphin, M., Boizet-Bonhoure, B., Descombes, P., Parker, K.L., Vassalli, J.-D., 2005. Gene expression during sex determination reveals a robust female genetic program at the onset of ovarian development. Dev. Biol. 287, 361-377.

Odet, F., Guyot, R., Leduque, P., Le Magueresse-Battistoni, B., 2004. Evidence for Similar Expression of Protein C Inhibitor and the Urokinase-Type Plasminogen Activator System during Mouse Testis Development. Endocrinology. 145, 1481-1489.

Ottolenghi, C., Pelosi, E., Tran, J., Colombino, M., Douglass, E., Nedorezov, T., Cao, A., Forabosco, A., Schlessinger, D., 2007. Loss of Wnt4 and Foxl2 leads to female-to-male sex reversal extending to germ cells. Hum. Mol. Genet. 16, 2795-2804.

Parma, P., Radi, O., Vidal, V., Chaboissier, M.C., Dellambra, E., Valentini, S., Guerra, L., Schedl, A., Camerino, G., 2006. R-spondin1 is essential in sex determination, skin differentiation and malignancy. Nat. Genet. 38, 1304-1309.

Perera, E.M., Martin, H., Seeherunvong, T., Kos, L., Hughes, I.A., Hawkins, J.R., Berkovitz, G.D., 2001. Tescalcin, a Novel Gene Encoding a Putative EF-Hand Ca2+-Binding Protein, Col9a3, and Renin Are Expressed in the Mouse Testis during the Early Stages of Gonadal Differentiation. Endocrinology. 142, 455-463.

Rahmoun, M., Lavery, R., Laurent-Chaballier, S., Bellora, N., Philip, G.K., Rossitto, M., Symon, A., Pailhoux, E., Cammas, F., Chung, J., Bagheri-Fam, S., Murphy, M., Bardwell, V., Zarkower, D., Boizet-Bonhoure, B., Clair, P., Harley, V.R., Poulat, F., 2017. In mammalian foetal testes, SOX9 regulates expression of its target genes by binding to genomic regions with conserved signatures. Nucleic Acids Res. 45, 7191-7211.

Robinson, M., Oshlack, A., 2010. A scaling normalization method for differential expression analysis of RNA-seq data. Genome Biol. 11, R25.

Robinson, M.D., McCarthy, D.J., Smyth, G.K., 2010. edgeR: a Bioconductor package for differential expression analysis of digital gene expression data. Bioinformatics. 26, 139-140.

Rolland, A.D., Lehmann, K.P., Johnson, K.J., Gaido, K.W., Koopman, P., 2011. Uncovering Gene Regulatory Networks During Mouse Fetal Germ Cell Development. Biol. Reprod. 84, 790-800.

Schmidt, D., Ovitt, C.E., Anlag, K., Fehsenfeld, S., Gredsted, L., Treier, A.-C., Treier, M., 2004. The murine winged-helix transcription factor Foxl2 is required for granulosa cell differentiation and ovary maintenance. Development. 131, 933-942.

Sekido, R., Lovell-Badge, R., 2008. Sex determination involves synergistic action of SRY and SF1 on a specific Sox9 enhancer. Nature. 453, 930-934.

Small, C.L., Shima, J.E., Uzumcu, M., Skinner, M.K., Griswold, M.D., 2005. Profiling Gene Expression During the Differentiation and Development of the Murine Embryonic Gonad. Biol. Reprod. 72, 492-501.

Smith, L., Van Hateren, N., Willan, J., Romero, R., Blanco, G., Siggers, P., Walsh, J., Banerjee, R., Denny, P., Ponting, C., Greenfield, A., 2003. Candidate testis-determining gene, Maestro (Mro), encodes a novel HEAT repeat protein. Dev. Dyn. 227, 600-607.

Spiller, C., Koopman, P., Bowles, J., 2017. Sex Determination in the Mammalian Germline. Annu. Rev. Genet. 51, 265-285.

Spiller, C.M., Feng, C.-W., Jackson, A., Gillis, A.J.M., Rolland, A.D., Looijenga, L.H.J., Koopman, P., Bowles, J., 2012. Endogenous Nodal signaling regulates germ cell potency during mammalian testis development. Development. 139, 4123-4132.

Stévant, I., Neirijnck, Y., Borel, C., Escoffier, J., Smith, L.B., Antonarakis, S.E., Dermitzakis, E.T., Nef, S., 2018. Deciphering Cell Lineage Specification during Male Sex Determination with Single-Cell RNA Sequencing. Cell Reports. 22, 1589-1599.

Stuart, J.M., Segal, E., Koller, D., Kim, S.K., 2003. A Gene-Coexpression Network for Global Discovery of Conserved Genetic Modules. Science. 302, 249-255.

Svingen, T., Koopman, P., 2013. Building the mammalian testis: origins, differentiation, and assembly of the component cell populations. Genes Dev. 27, 2409-2426.

Torres, M., Gomez-Pardo, E., Dressler, G.R., Gruss, P., 1995. Pax-2 controls multiple steps of urogenital development. Development. 121, 4057-4065.

Tsuda, M., Sasaoka, Y., Kiso, M., Abe, K., Haraguchi, S., Kobayashi, S., Saga, Y., 2003. Conserved Role of nanos Proteins in Germ Cell Development. Science. 301, 1239-1241.

Uda, M., Ottolenghi, C., Crisponi, L., Garcia, J.E., Deiana, M., Kimber, W., Forabosco, A., Cao, A., Schlessinger, D., Pilia, G., 2004. Foxl2 disruption causes mouse ovarian failure by pervasive blockage of follicle development. Hum. Mol. Genet. 13, 1171-1181.

Uhlenhaut, N.H., Jakob, S., Anlag, K., Eisenberger, T., Sekido, R., Kress, J., Treier, A.-C., Klugmann, C., Klasen, C., Holter, N.I., Riethmacher, D., Schutz, G., Cooney, A.J., Lovell-Badge, R., Treier, M., 2009. Somatic sex reprogramming of adult ovaries to testes by FOXL2 ablation. Cell. 139, 1130-1142.

Ungewitter, E.K., Yao, H.H.C., 2013. How to Make a Gonad: Cellular Mechanisms Governing Formation of the Testes and Ovaries. Sex. Dev. 7, 7-20.

Vainio, S., Heikkila, M., Kispert, A., Chin, N., McMahon, A.P., 1999. Female development in mammals is regulated by Wnt-4 signalling. Nature. 397, 405-409.

Vidal, V.P.I., Chaboissier, M.-C., de Rooij, D.G., Schedl, A., 2001. Sox9 induces testis development in XX transgenic mice. Nat. Genet. 28, 216-217.

Wilhelm, D., Martinson, F., Bradford, S., Wilson, M.J., Combes, A.N., Beverdam, A., Bowles, J., Mizusaki, H., Koopman, P., 2005. Sertoli cell differentiation is induced both cell-autonomously and through prostaglandin signaling during mammalian sex determination. Dev. Biol. 287, 111-124.

Wilhelm, D., Washburn, L.L., Truong, V., Fellous, M., Eicher, E.M., Koopman, P., 2009. Antagonism of the testis- and ovary-determining pathways during ovotestis development in mice. Mech. Dev. 126, 324-336.

Yao, H.H., Matzuk, M.M., Jorgez, C.J., Menke, D.B., Page, D.C., Swain, A., Capel, B., 2004. Follistatin operates downstream of Wnt4 in mammalian ovary organogenesis. Dev. Dyn. 230, 210-215.

Yao, H.H., Whoriskey, W., Capel, B., 2002. Desert Hedgehog/Patched 1 signaling specifies fetal Leydig cell fate in testis organogenesis. Genes Dev. 16, 1433-1440.

Zhang, B., Horvath, S., 2005. A general framework for weighted gene co-expression network analysis. Stat. Appl. Genet. Mol. Biol. 4, Article17.

Zhao, S., Fung-Leung, W.P., Bittner, A., Ngo, K., Liu, X., 2014. Comparison of RNA-Seq and microarray in transcriptome profiling of activated T cells. PLoS One. 9, e78644.

Zhao, S., Xi, L., Zhang, B., 2015. Union Exon Based Approach for RNA-Seq Gene Quantification: To Be or Not to Be? Plos One. 10, e0141910.

Zimmermann, S., Schottler, P., Engel, W., Adham, I.M., 1997. Mouse Leydig insulin-like (Ley I-L) gene: structure and expression during testis and ovary development. Mol. Reprod. Dev. 47, 30-38.

Figure Legends

Fig. 1. Experimental time course. Mouse fetal gonadal transcriptomes were analyzed using RNA-Seq from 10.5 to 13.5 dpc. This time window includes formation of the bi-potential genital ridge (10.5 dpc), sex determination (11.5 dpc), and fetal testis and ovary differentiation (12.5 and 13.5 dpc).

Fig. 2. Validation of the RNA-Seq data. Graphs indicate deduced expression of several marker genes from the RNA-Seq data; in all cases consistent with previous reports. Error bars, standard deviation.

Fig. 3. Identification of genes expressed in a sexually dimorphic manner. (A) Stack bar chart showing numbers of sex-biased genes on X, Y, or autosomes from 10.5 to 13.5 dpc. Total numbers of sex-biased genes are shown above each bar. (B) Venn diagrams comparing male- or female-biased genes identified at 11.5, 12.5 or 13.5 dpc.

Fig. 4. *Gm10352*, a Y-linked gene, may be co-regulated with *Sry* in XY genital ridges. (A) Expression graph of Gm10352 from the RNA-Seq data showing a transient expression peak at 11.5 dpc, mirroring the expression profile of *Sry* (see Figure 2). (B) *Gm10352* is located ~250 kb upstream of *Sry*. Arrows indicate the transcriptional orientation.

Fig. 5. Identification of temporally regulated genes. (A) Bar chart showing numbers of temporally regulated genes between consecutive time points in XX or XY fetal gonads. (B) Venn

diagrams comparing up- or down-regulated genes in XX and XY gonads during each 1-day interval across the time course. (C) *Gata4* and *Lhx9* were up-regulated in both XX and XY gonads from 10.5 to 11.5 dpc. (D) *Osr1* and *Pax2* were down-regulated in both XX and XY gonads from 10.5 to 11.5 dpc.

Fig. 6. Relative contribution of transcriptional activation and repression to sexually dimorphic gene expression varies with time. Venn diagrams comparing genes manifesting biased expression in one sex, those up-regulated in the relevant sex, and those down-regulated in the opposite sex.

Fig. 7. Co-expression gene network analysis of mouse fetal gonadal development. Heatmap showing relative expression of genes in 5 representative sex- and/or stage-specific gene modules across all samples. Module names with representative member genes are shown on the left and the deduced associated functions on the right.

Fig. 8. Widespread alternative splicing and its regulation in the developing gonads. Global identification of differentially spliced exonic regions. (A) Pie chart showing numbers and percentages of genes expressing various numbers of transcript isoforms. (B) Stack bar chart showing sex-biased splicing events on X, Y, or autosomes from 10.5 to 13.5 dpc. Total numbers of exonic regions are shown above each column. (C) Venn diagram showing limited overlap of sex-biased splicing events identified at 11.5, 12.5 or 13.5 dpc. (D) Bar chart showing numbers of

temporally-regulated splicing events between consecutive time points in either XX or XY fetal gonads.

Fig. 9. Combined regulation of *Lef1* splicing and transcription during fetal ovarian development. (A) Scatter plot showing significant increase of exon 6 inclusion in XX gonads between 10.5 and 12.5 dpc, leading to the female-biased inclusion of exon 6 at 12.5 and 13.5 dpc. Each symbol represents a pairwise comparison, either between two consecutive time points in XX (circles) or XY (squares), or between XX and XY at the same time point (diamonds). Shaded symbols indicate statistical significance. The horizontal dotted line indicates the *P* value cut-off of 0.05, while the vertical dotted lines indicate the $\log_2$ fold change cut-off of 1 or -1. (B) Exon 6 (indicated with a green arrow) of *Lef1* was differentially spliced between XX and XY at 13.5 dpc. Top panel: DEXSeq fitted exon usage values of each exonic regions according to the generalized linear model (with overall changes in gene expression subtracted); bottom panel: flattened gene model and annotated transcript isoforms of *Lef1*. (C) BigWig read coverage plots showing significantly more sequencing reads mapped to exon 6 of *Lef1* in XX than XY gonads at 13.5 dpc. In the plots, height at each genomic position represents the depth of uniquely mapped sequencing reads. The inclusion of exon 6 generates a transcript isoform encoding the full-length LEF1 protein, whereas the skipping of exon 6 generates a shorter isoform encoding LEF1*. (D) Expression graph of *Lef1* from RNA-Seq data showing significantly higher expression levels in XX gonads than XY at 12.5 and 13.5 dpc.

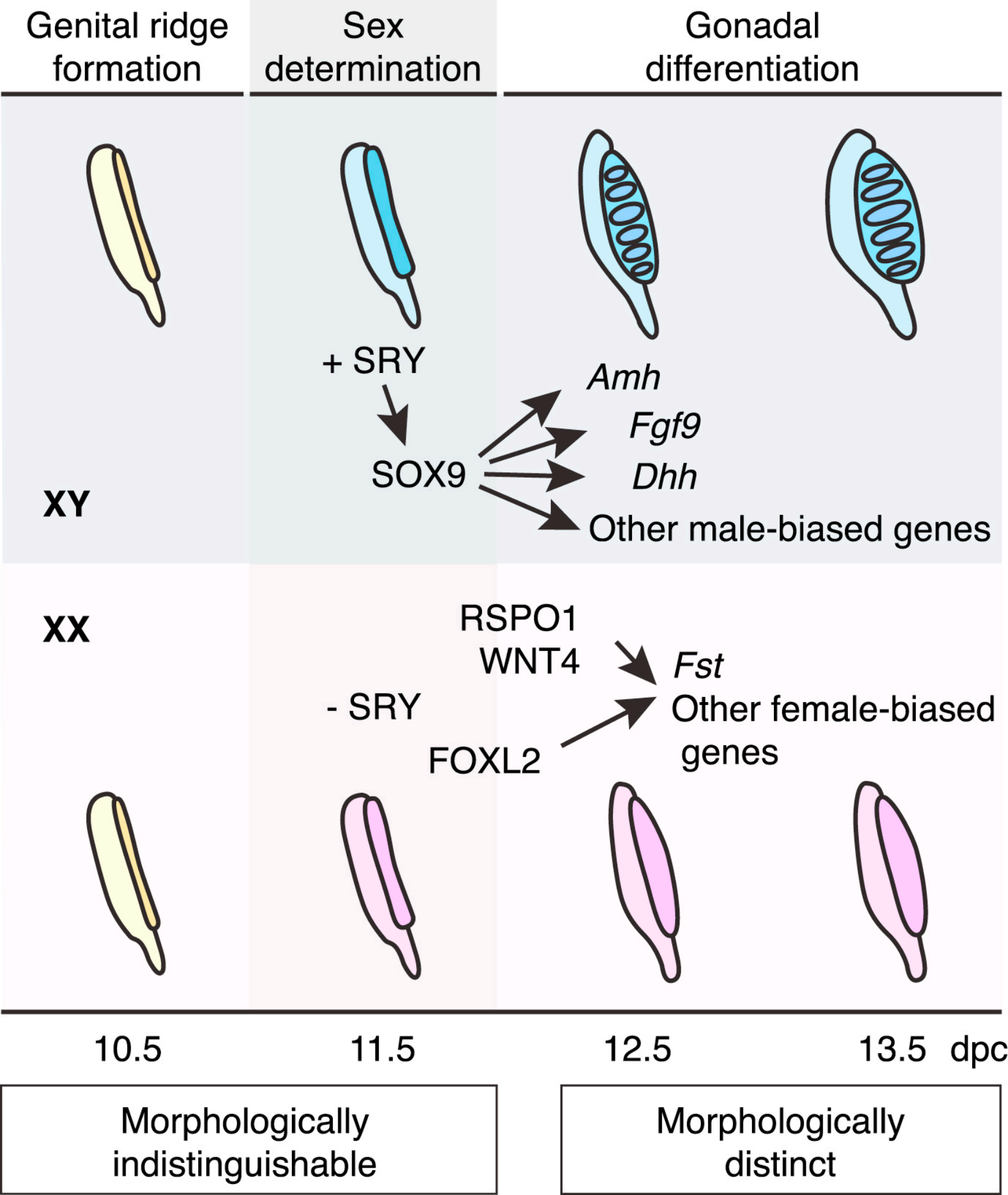
Genital ridge formation
Sex determination
Gonadal differentiation
+ SRY
SOX9
Amh
Fgf9
Dhh
Other male-biased genes
XY
XX
RSPO1
WNT4
Fst
- SRY
Other female-biased genes
FOXL2
10.5
11.5
12.5
13.5 dpc
Morphologically indistinguishable
Morphologically distinct

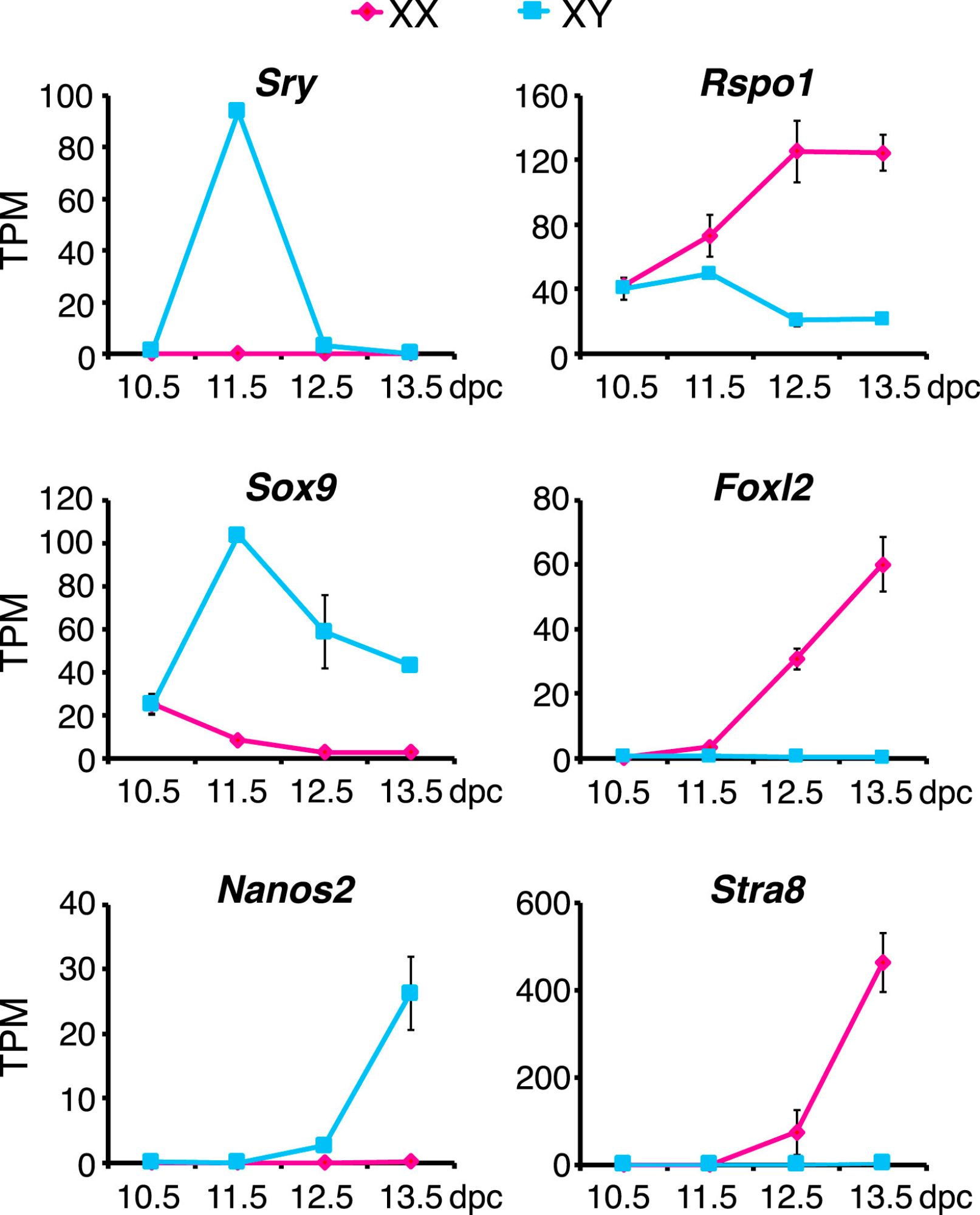
XX
XY
Sry
Rspo1
Sox9
Foxl2
Nanos2
Stra8
TPM
100
80
60
40
20
0
160
120
120
40
30
10
600
400
200
10.5
11.5
12.5
13.5 dpc

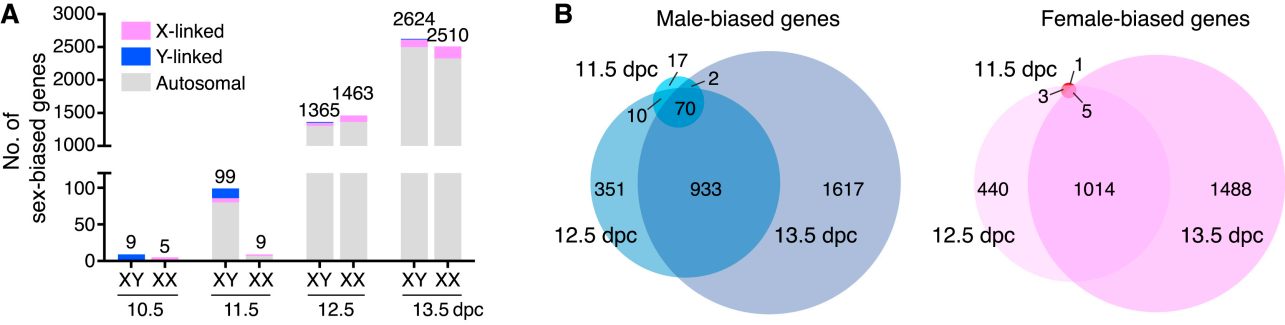
A
No. of sex-biased genes
3000
2500
2000
1500
1000
100
50
0
X-linked
Y-linked
Autosomal
9
5
99
9
1365
1463
2624
2510
XY XX XY XX XY XX XY XX
10.5
11.5
12.5
13.5 dpc
B
Male-biased genes
11.5 dpc
17
2
10
70
351
933
1617
12.5 dpc
13.5 dpc
Female-biased genes
11.5 dpc
1
3
5
440
1014
1488
12.5 dpc
13.5 dpc

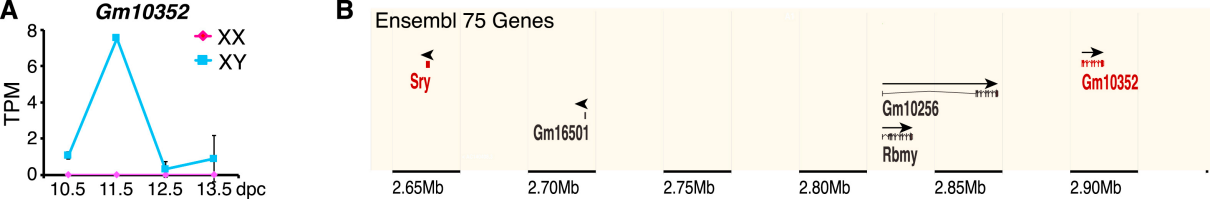
A
Gm10352
XX
XY
TPM
8
6
4
2
0
10.5
11.5
12.5
13.5 dpc
B
Ensembl 75 Genes
Sry
Gm16501
Gm10256
Rbmy
Gm10352
2.65Mb
2.70Mb
2.75Mb
2.80Mb
2.85Mb
2.90Mb

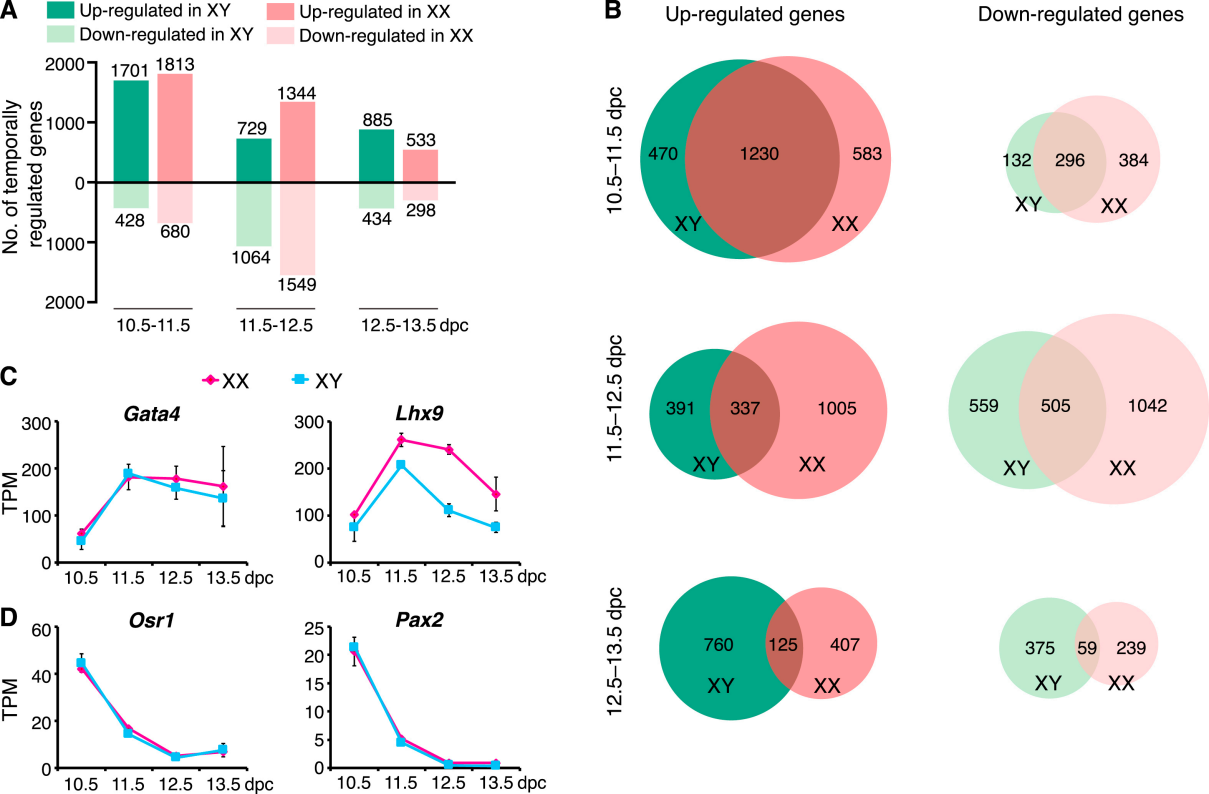
A
Up-regulated in XY
Down-regulated in XY
Up-regulated in XX
Down-regulated in XX
No. of temporally regulated genes
2000
1000
0
1000
2000
1701
1813
428
680
729
1344
1064
1549
885
533
434
298
10.5-11.5
11.5-12.5
12.5-13.5 dpc
B
Up-regulated genes
Down-regulated genes
10.5–11.5 dpc
470
1230
583
XY
XX
132
296
384
XY
XX
11.5–12.5 dpc
391
337
1005
XY
XX
559
505
1042
XY
XX
12.5–13.5 dpc
760
125
407
XY
XX
375
59
239
XY
XX
C
XX
XY
Gata4
Lhx9
TPM
300
200
100
0
10.5
11.5
12.5
13.5 dpc
D
Osr1
Pax2
TPM
60
40
20
0
25
20
15
10
5
0
10.5
11.5
12.5
13.5 dpc

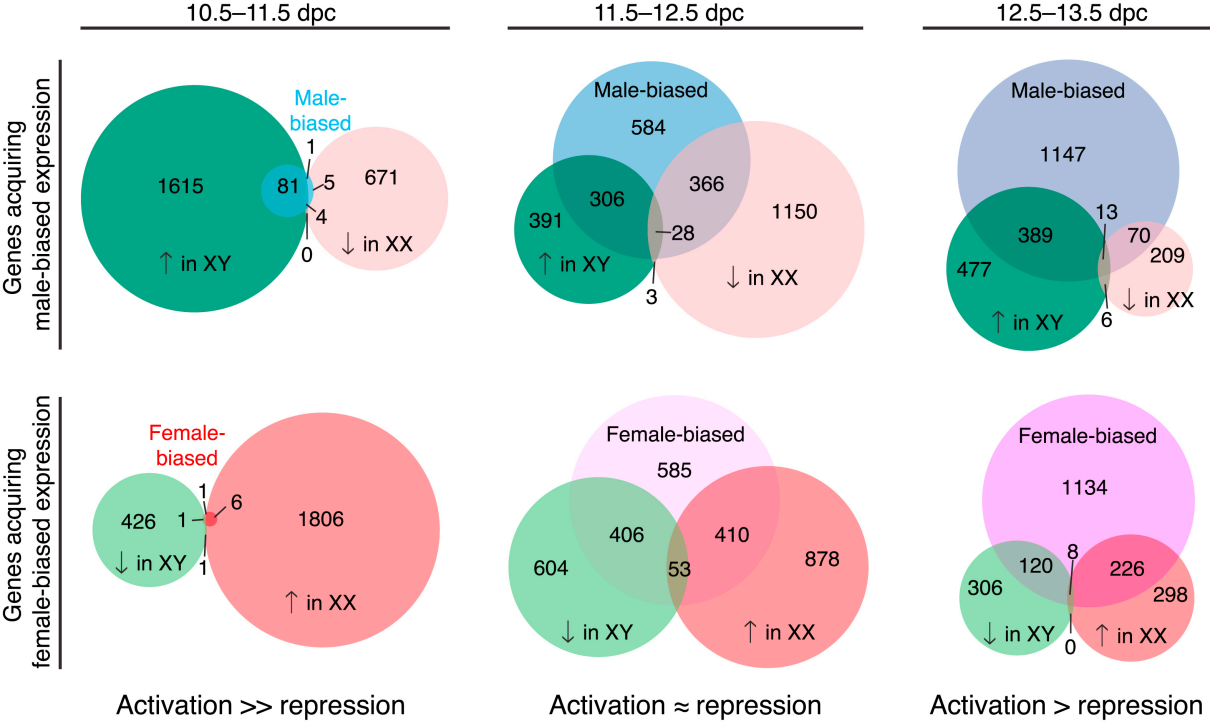
10.5–11.5 dpc
11.5–12.5 dpc
12.5–13.5 dpc
Genes acquiring male-biased expression
Genes acquiring female-biased expression
Male-biased
1615
81
1
5
4
0
671
↑ in XY
↓ in XX
Male-biased
584
306
366
391
28
1150
↑ in XY
3
↓ in XX
Male-biased
1147
13
389
70
209
477
↑ in XY
6
↓ in XX
Female-biased
1
6
426
1
1806
↓ in XY
1
↑ in XX
Female-biased
585
406
410
604
53
878
↓ in XY
↑ in XX
Female-biased
1134
8
120
226
306
298
↓ in XY
0
↑ in XX
Activation >> repression
Activation ≈ repression
Activation > repression

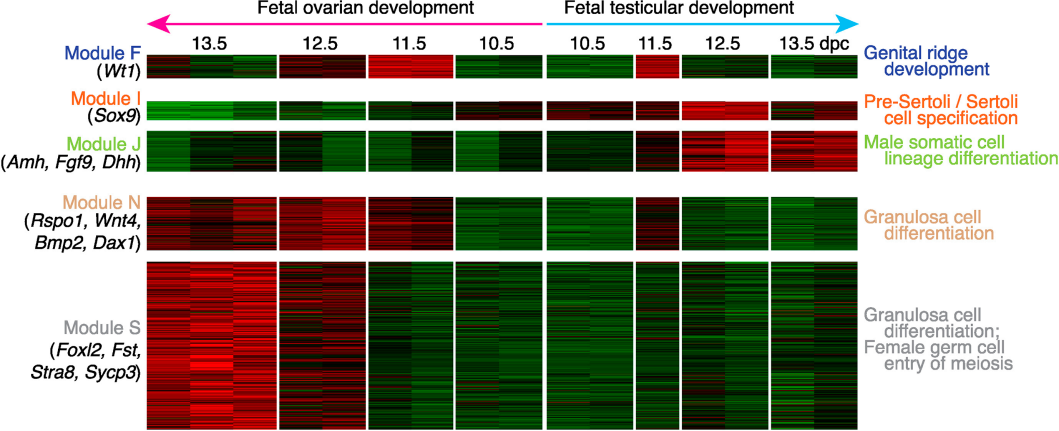
Fetal ovarian development
Fetal testicular development
13.5
12.5
11.5
10.5
10.5
11.5
12.5
13.5 dpc
Module F
(Wt1)
Genital ridge
development
Module I
(Sox9)
Pre-Sertoli / Sertoli
cell specification
Module J
(Amh, Fgf9, Dhh)
Male somatic cell
lineage differentiation
Module N
(Rspo1, Wnt4,
Bmp2, Dax1)
Granulosa cell
differentiation
Module S
(Foxl2, Fst,
Stra8, Sycp3)
Granulosa cell
differentiation;
Female germ cell
entry of meiosis

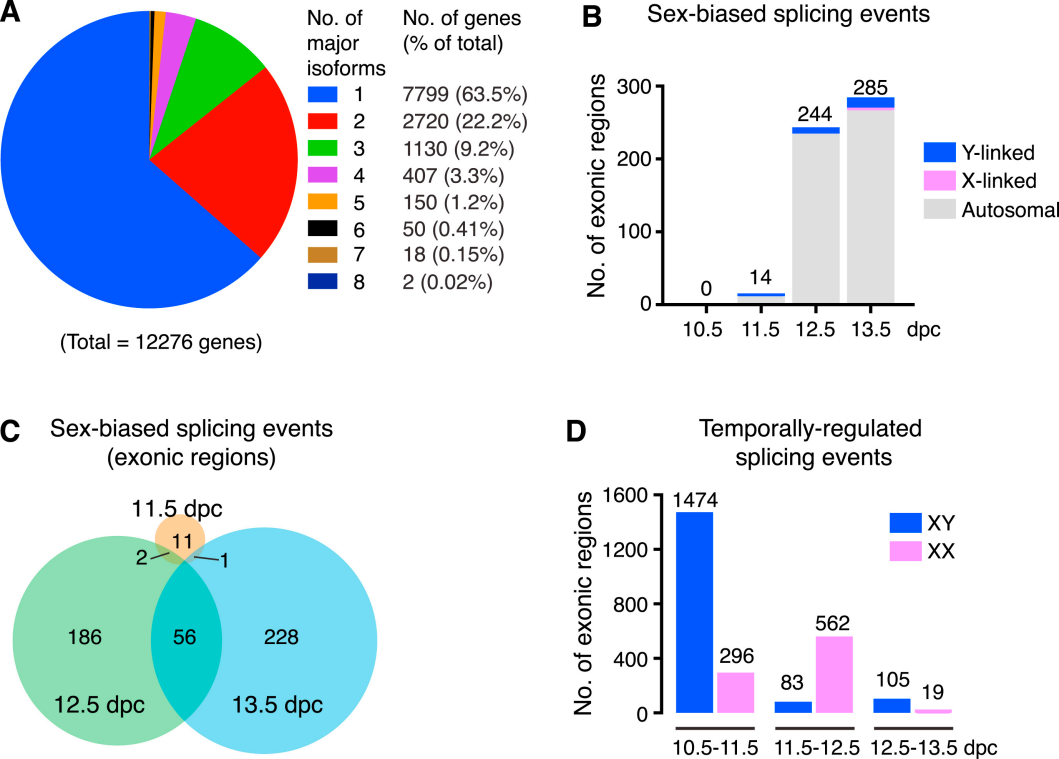
A
No. of major isoforms
No. of genes (% of total)
1 7799 (63.5%)
2 2720 (22.2%)
3 1130 (9.2%)
4 407 (3.3%)
5 150 (1.2%)
6 50 (0.41%)
7 18 (0.15%)
8 2 (0.02%)
(Total = 12276 genes)
B
Sex-biased splicing events
No. of exonic regions
300
200
100
0
0
14
244
285
10.5
11.5
12.5
13.5
dpc
Y-linked
X-linked
Autosomal
C
Sex-biased splicing events (exonic regions)
11.5 dpc
11
2
1
186
56
228
12.5 dpc
13.5 dpc
D
Temporally-regulated splicing events
No. of exonic regions
1600
1200
800
400
0
1474
296
83
562
105
19
XY
XX
10.5-11.5
11.5-12.5
12.5-13.5 dpc

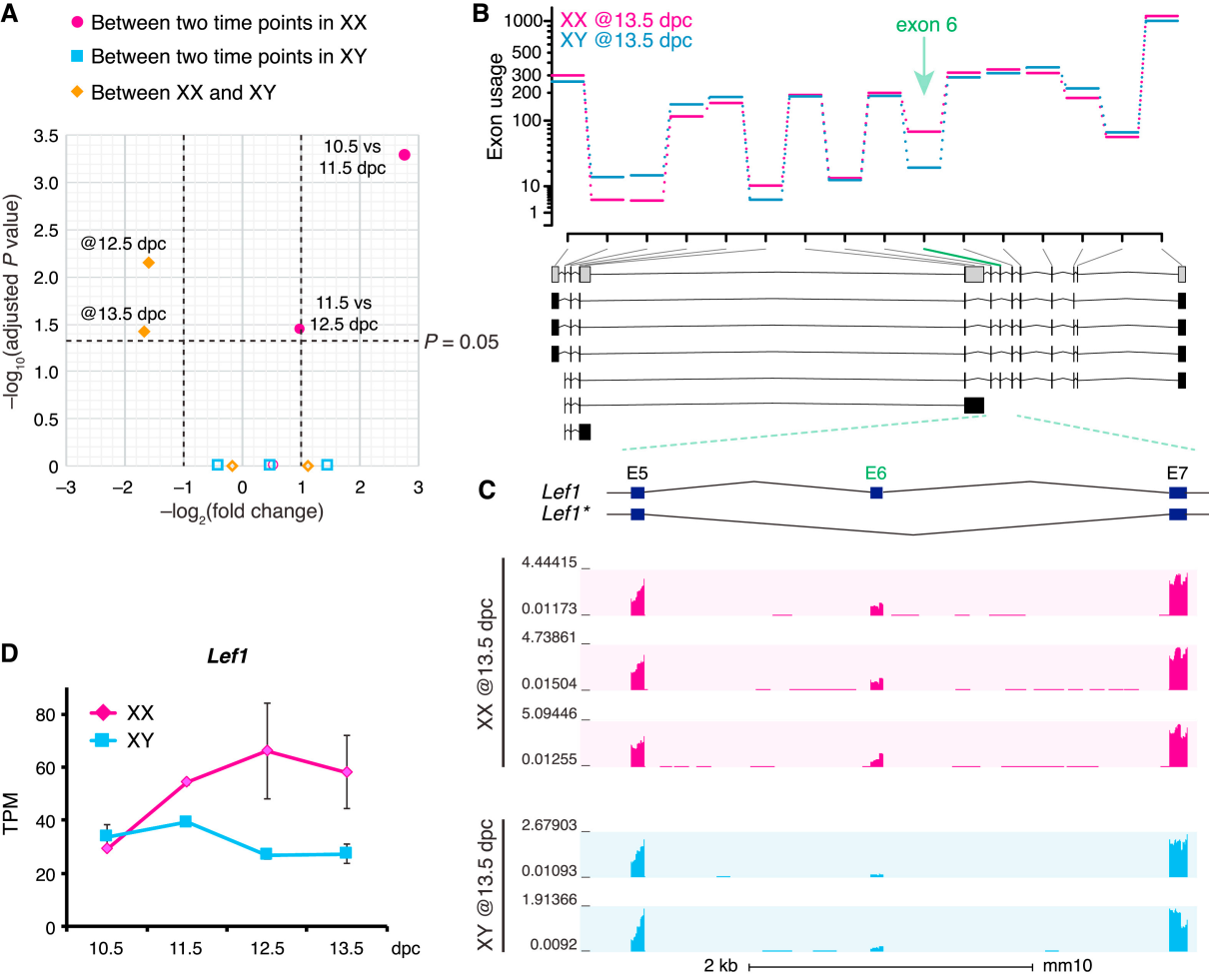
A
Between two time points in XX
Between two time points in XY
Between XX and XY
10.5 vs 11.5 dpc
@12.5 dpc
@13.5 dpc
11.5 vs 12.5 dpc
P = 0.05
−log10(adjusted P value)
−log2(fold change)
B
XX @13.5 dpc
XY @13.5 dpc
exon 6
Exon usage
C
Lef1
Lef1*
E5
E6
E7
XX @13.5 dpc
XY @13.5 dpc
4.44415
0.01173
4.73861
0.01504
5.09446
0.01255
2.67903
0.01093
1.91366
0.0092
2 kb
mm10
D
Lef1
XX
XY
TPM
dpc

- Transcriptomic & spliceomic dataset for mouse sex determination and gonadogenesis

- Co-expression cohorts identify new candidates for sex development and sex disorders

- The role of splicing regulation in this system may have been underappreciated